'The summertime Saharan heat low: Sensitivity of the radiation budget and atmospheric heating to water vapour and dust aerosol' by Netsanet K. Alamirew et al

Response to referees and reviewer

Formatted: Left

The comments and suggestions made by all referees and reviewer are useful. We have addressed the comments raised. Our responses and changes (if any) are indicated in the corrected version of the paper. For clarity we put original comment of the reviewer (typed in italic font) followed by our responses to make it easy to follow.

Response to interactive discussion Short Comment (SC) from C. Lavaysse

Major Comment a.

1. *Section 3 is not clear. Quite complicated to understand all the configurations and the conclusions drawn from these results on the choice of certain parameters. Finally choices are not really justified and I am not sure if it is necessary to provide all the information. I would recommend to simplify this section and to put some results in the supplementary material.*

Response

Part of section 3 has been moved to the supplementary material (Section S2). This includes all the model configuration analysis. Accordingly, Section 3 now describes the data and the design of the hypothesis testing experiments and Section 4 focuses only on the results of those experiments.

Changes Made

We have reorganized section 2 and 3 into a more clear structure. The new structure of the whole paper is as follows.

Section 1. Introduction
Section 2. Description of RT model
Section 3. Data and method
- 3.1. Observed top of atmosphere and surface radiation measurements
- 3.2. Atmospheric profile and surface characteristics
- 3.3. Dust properties and extinction profile
- 3.4. RT model Experiments

Section 4. Results and discussions.
- 4.1. RT model validation
- 4.2. The radiative flux and heating effects of dust and water vapour
  - 4.2.1. Dust

4.2.2. Water vapour

4.2.3. The relative effects of dust versus water vapour

Section 5. Summary and Conclusions

Original draft Page 6:L19-40, Page 7:L1-3, Page 7:L28-37 moved to supplementary material (section S2). See also minor comment #3.

2. *In this section I also found some parts not clear: p5 l5-12; it is quite weird to compare observations assimilated with model dataset? The authors do not explain the remaining errors. Is it due to the assimilation procedure?*

Response

We are pointing the fact that despite assimilation of the radiosonde data there remain biases in the reanalysis. Fennec was a short-term experiment and since then there remains only one radiosonde station for the whole Sahara. As such, the reanalysis errors we derive are almost certainly much lower than those typical of the rest of the Sahara. We also now cite the errors estimated from Garcia-Carreras who compared radiosonde data to a forecast model first guess (independent of assimilation)
The magnitude of errors are different among the different reanalysis products. The possible reasons for the remaining error between observation and reanalysis products could be due to differences in models core dynamics and in assimilation procedures.

Changes Made

Corrected draft Page 4. L36-38. A statement added suggesting the possible reasons for differences in error among reanalyses.

Major Comment b.

1. *Section 4 is too descriptive with too much information that are not necessarily significant or important to the conclusions of this study. This is particularly true p9 and 10. I strongly recommend to reduce this part to the most important results and to put the others results into an annex.*

Response

Part of section 4 has been moved to the supplementary Material (section S3), specifically sections describing the sensitivity experiments towards the model optimum configuration, as we agree these are not the key significant results.

We choose to retain some of the results originally presented in pages 9-10 because we feel it is important to demonstrate that the simulated quantities of top of atmosphere radiation budgets are within the observational uncertainties. To give sense of results in subsequent sections, it is necessary to have a feeling of the surface and TOA radiative budget under the mean state.

Changes Made

Original draft page 8:L30-33, page 9:L3-8 moved to supplementary material (section S3)

2. *The summary of the subsection 4.1 is too speculative. How the authors can conclude the simulated flux errors of the optimal configuration are comparable to the observational uncertainties? What does 'acceptable' mean?*

Response

Given that we do not have accurate data for all the input required to run the RT model, it is not unexpected to get some uncertainty in our results. However we have chosen the inputs in such a way that the calculated flux are as close as possible to observation. This is what we mean by an 'optimum' model configuration. The optimum configuration is deemed to be 'acceptable' because the model error in top of atmosphere fluxes (perhaps the single most important quantity) with respect to observations is within the uncertainty in the observational estimates of those quantities. Model estimates lying within observation range is a commonly used indicator of acceptable model performance. Thus we suggested the RT model is configured to produce acceptable results and thus can be used for further experiments.

Major Comment c.

1. *Some conclusions are too speculative. The authors conclude about the impacts of the dust aerosols and water vapor on the SHL but, in that study, only June 2011 is used. The SHL is the most important from end of June to mid of September (when it is installed in its Saharan location). Even if the authors used only one month (June), they have to characterize this specific year to the climatology (in term of dust, humidity, large scale forcings). This point concerns the title ('summertime' is not appropriate), the conclusions (p15 l8-10), and the abstract.*

Response

We agree that the period of study does not coincide with the peak of the summer season when the SHL is established in its northernmost position. However, we are limited by the period of the Fennec field campaign whose data underpin our analysis. Accordingly we have changed all references to 'summertime' to 'early summer'. In addition, in Section 3.2 we note that during our study period of June 2011 the SHL underwent a rapid transition from a 'maritime phase' to a 'heat low' phase. As such our analysis actually covers the transition period and SH states characteristic of both early and high summer. We have now amended this section to include an analysis of the conditions during June 2011 with respect to the mean conditions during June.

Changes Made

References to summer changed to summertime.

Figure 1 changed to show position of SHL in June, 2011.

Corrected draft Page 16:L14-20. A paragraph added

2. *Also the discussion on the impacts on the SHL pulsations should be carefully discussed since the authors do not analyze the contribution of the large scale temperature advections and they never show the real position of the SHL in June 2011 (in June, the SHL is migrating to the north with a large spatial variability).*

Response

Real position of SHL in June is shown in Fig 1.

The comments on our reference to variability in SHL specifically the 'pulsating' of SHL intensity and the potential role of dust and water vapour feedbacks in this process is also raised by anonymous referee #1. We do feel it is important in this paper to relate the radiative heating rates derived from our RT simulations to the behaviour of the SHL, but of course recognise that the full dynamical response requires an analysis of advective heating. As such in the original paper p16 para 1 we note that radiative heating is of 'comparable magnitude' to published estimates of advective cooling from comparable monsoon surge type events. In this way we make only a broad inference about the net effects of advective and radiative terms on the SHL. We have now changed the text slightly to emphasise the speculative nature of this inference.

Changes Made

Corrected draft Page 15:L26-28. Additional statement included.

'

3. *Finally at climatological scale, the authors should pay attention to the climatological evolution of the dust that tends to reduce (p15 l16)*

Response

Our comment in the original draft page 15:L16 concerns other analysis which implicate long term trends in SHL temperature to that in WV, but do not include dust in their analyses. We simply aimed to point out that this should not be neglected. Our paper is not concerned with resolving long term trends in dust over the SHL so we do not include plots of long term satellite derived AOD over the SHL.

Major Comment d.

1. *Some figures are not readable*

Response

Unreadable figures corrected.

Minor Comments

1. *P2 l11 the authors should mention this reference: Lavaysse, C., Flamant, C., Evan, A. et al. Clim Dyn (2016) 47: 3479. doi:10.1007/s00382-015-2847-z*

   Response: Reference included, P2:L11 and reference section page 18: L32.

2. *P6 l4; the two phases mentioned are not so clear.*

   Response: These two phases are previously stated on original draft page 4:L40 and page 5:L1

3. *P6 l19: title of subsection 3.2 not clear, please rephrase*

   Response: changed to 'RT sensitivity experiments to choice of inputs', now moved to supplementary material.

4. *P6 l24: optimal to what?*

   Response: Optimal configuration means model configured to produce results closest to observations.

5. *P6 l37-38; how do the authors conclude the Ceres measurements are uncertain and that explain the large RMSE? The term RMSE refers to a reference (usually observations) that are considered as the correct value. Here, I do not understand what is the reference and how they can conclude that. Please clarify. Also the term RMSD (difference) should be more appropriate.*

   Response: We do agree with the reviewer's comment that RMSD is comparison of modeled versus observation. From the data we have CERES is considered correct, despite its limitations as with any observation, can be used to measure the error modelled variables.

   Changes Made: RMSE changed to RMSD in all occasions.

6. *P6 l39-40: the authors provide some results without explanations, what are these results (mean =...) and please clarify the conclusions/interest of this point?*

   Response: Rephrased, point of interest described in section 5

7. *P7 subsection 3.2.2 I recommend to put the first part of the paragraph in the introduction section and the result in supplementary material.*

   Response: Some of the information and results on optical properties of dust is now moved to section S1 of supplementary material.

8. P8 l1: Section 4.1 is correct?

   Response: Corrected

9. *P8 l11: Is it necessary to use this acronym?*

   Response: Acronym definitions summarized in table 2. To be consistent throughout the paper, we found it necessary to use acronym.

10. *P8 l27: Section 3.1 is correct?*

Response: corrected, for the details look at response to Major comment a.

11. *P11 l7-8: longwave and shortwave are equal*

Response: TOA SW DRE of dust is small, whereas LW has a net warming effect at TOA(less LW escaping out of atmosphere due to dust.)

12. *P12 l36-37: The SHL is measured in between 925 and 700hPa, not at the surface. Do the authors conclude there is a cooling of the SHL intensity due to the water vapor?*

Response: Here we are discussing the immediate radiative effect of dust and water vapour. But the net effect may not be cooling as the feedback resulting from surface warming in the LW and thus more sensible heat flux could result in net warming of the atmosphere which needs further investigation using regional climate models that include the feedback processes.

13. *Figures : For all the figures, please add the caption under the figures*

Response: All changes are made to the figures according to the given recommendation.

Response to Referee Comment (RC) from Anonymous Referee #1

1. *This paper used field experiment data at BBM in southern Algeria from June 2011 and a radiative transfer model to calculate the effects of dust and water vapor on radiation budget both at the surface and the TOA in order to understand the radiative processes within the SHL during summer. Generally, the manuscript is straightforward and well organized. However my main concern is that some of the input data for the RT model may cause large uncertainties that are helpless to fill the research gaps as the authors mentioned in the introduction.*

Response

We fully recognise the challenge of adequately constraining the input data to the RT model in this region, where observations are sparse and as a results reanalyses models have limited assimilation of observations. This is indeed a challenge and one which the Fennec project set out to address. In using Fennec data we therefore utilise the best available data for our RT simulations. Moreover, we undertake a very comprehensive analysis of the sensitivity of radiative heating to uncertainties in those input field not directly measured during Fennec. Indeed reviewer 1 felt that this model configuration section was too comprehensive to be included in the main paper! So we believe we have addressed the issue of data input uncertainty as thorough and comprehensive manner as could be reasonably expected. This is now included in the supplementary material section so as not to distract from the core hypotheses the paper sets out the test.

2. *For example, dust can absorb thermal infrared radiation, the night time AOD estimated from the nephelometer, which measures aerosol extinction coefficient near the surface, could induce a large error without an accurate aerosol extinction profile.*

Response

Lack of complete input data is one of the challenges in the study of radiative effect of aerosols. Because of this, there is always assumptions or approximations to overcome the arising difficulties. Using surface nephelometer measurements to estimate night time AOD will not significantly affect our result. This is because there is only LW forcing at night which is in general smaller compared with SW forcing. Besides researchers practically use uniform dust extinction profile across the boundary layer as the difference in forcing results compared with the actual extinction profile is not small. [Liao and Seinfeld 1998, Osipov et al., 2015,]

We have also confirmed this through a sensitivity experiment to test the difference in LW radiative flux and heating rate when we use different daytime and nighttime extinction profile. We find a small difference less than 3 $W.m^{-2}$ both at the surface and TOA. The atmospheric heating rates do not change significantly when different extinction profiles are used for day and night except small difference in the lower levels by less than 0.20 $K\ day^{-1}$. We conclude in general that this will not affect what we wanted to show and hence the overall result of the paper.

3. *Reanalysis data generally has poor representations of clouds and their properties. However, the authors selected clouds properties from the reanalysis. These could directly affect the reliability of the model results.*

Response

This was also our concern at the beginning of this research work as we understand the limitations of cloud representations in models. We could have undertaken the RT experiments only in clear sky mode as many other authors choose to do. We do include clear sky only experiments but we complement these with all sky experiments to provide a more thorough and comprehensive analysis, from which we compare observations of TOA fluxes in which cloud screening is problematic. Our all sky RT experiments use what we feel is the best available 3-D information on cloud, that comes from the reanalysis models. Alternative cloud profiles for RT models simulations is not available. It is totally expected that our results will bring error due to cloud under (or mis) representation. We discuss this on Page 9: L14-20 of corrected draft and page 3:L1-5, L14-16 of supplementary material. However, we stand by our analysis not least because comparison of the errors in the all sky vs clear sky RT results actually provide some first order indication of the error on radiative budget due to underestimated cloud in reanalysis dataset. We have included a clearer and more explicit caveat regarding the limitations of the cloud fields in our experiments and note the need for further work in this area.

Changes Made

Page 3:L14-16 of supplementary material.

4. *Sections 2 and 3 are a bit long. I would recommend to combine and simplify this part.*

Response

This part has been restructured in a more clear way (please refer to the comment of reviewer 1, reviewer #1 Major Comment a #1.)

Changes Made

Refer to the response of reviewer #1 Major Comment a #1 for the simplified layout of the paper.

5. *What the authors concluded cannot be totally supported only from the radiative forcing and heating rate calculations.*

Response

Reviewer #1 also raised this comment. Please refer the responses made to reviewer #1, Major Comment C #2

6. *The manuscript also need a thorough editing. Some typos and confusing expression make the text difficult to follow at times.*

Response

Manuscript thoroughly read and corrections made to typos.

Response to Referee Comment (RC) from Anonymous Referee #2

Major Comments

1. *Error Analysis: The authors spend a good bit of time estimating uncertainty in their modeled fluxes via comparison to satellite retrieved fluxes. However, when it comes to the data analysis, these uncertainties are not taken into consideration. I think it's great that the authors have a handle on the RT model errors, but I think it would be far more useful to carry those uncertainties throughout the entirety of Section 4. Doing so would make the paper and results much stronger and would afford the community opportunity to make a more precise comparison between yours and future dust forcing estimates.*

Response

We agree the importance of including error analysis despite we have reduced the uncertainty using

sensitivity experiments. This is addressed qualitatively to some extent in section 4, i.e. error associated with the uncertainties in the input.

Changes made

Additional information quantitatively expressing the error in flux calculation associated with uncertainties in some of the input data is provided. Page 8 L25-28 and L37-39.

2. *Radiative Transfer Model. To generate the mie coefficients the authors use two different size distributions (Dubovik and Ryder) but the same index of refraction. However, what's the source of the refractive index? The authors conclude that the Dubovik size distribution is more representative of the actual size distribution based on a comparison of the model and observed/retrieved fluxes. However, it is completely possible that the index of refraction used here also biased. For example, it's possible that the Ryder distribution is correct but doesn't produce enough SW dust forcing because the MEC is too low at the appropriate size parameter, thus the forcing in the SWE for Dubovik would better match observations because it's biased towards smaller particles. At any rate, my only point is that you have two degrees of freedom and you can't say conclusively that one size distribution is more representative than another one b/c the index of refraction isn't constrained.*

Response

We agree that the refractive index may cause uncertainty in the flux calculations especially in the SW absorption. It is also interesting to test the sensitivity of radiative flux to refractive index. In general for a given size distribution of dust, when refractive index is increased net SW heating will increase and net LW cooling will increase to a lesser extent. This however is a complicated function depending on the surface albedo and cloud. (Liao et al., 1998). Here we used recent measurements for dust refractive index over the Sahara (Ryder et al., 2013) which is function of the composition of dust particles, independent of the size distribution. It could be possible that if we reduce the refractive index, the SW heating will reduce in Ryder distribution, which is the biggest discrepancy compared with satellite measurement. But we haven't made sensitivity test as we have measured refractive index.

3. *RT Model: The authors state that the vertical profile of the dust mass mixing ratio is adjusted so that for a given MEC the AOD matches observations. Is the profile linearly scaled by a single value to match the observations? Is a single coefficient derived for all cases or is this done independently for each RT simulation?*

Response

To be clearer, first an average extinction profile is derived from CALLIOP and this profile is used to derive the extinction profile at each time step, i.e. the average profile is adjusted to match the measured

AOD from AERONET. So to answer the question, for each RT calculations independent extinction profile is derived.

4. *Flux comparisons: It the text it is not clear if the flux comparisons are performed in a robust manner. For example, why are monthly mean fluxes from CERES compared to the observations and output from the model? The proper way to conduct the comparison with CERES would be to access the daily nighttime and daytime data and then sub sample the observations/RT model output/GERB retrievals in order to conduct an apples-to-apples comparison. The authors acknowledge this (Page 9 line 35) so it's puzzling why a more thorough analysis wasn't performed. This approach includes the task of making comparisons to the reanalysis data (again, authors note that interpolating MERRA surface temperature may be biasing the flux comparisons). Furthermore, more insight would likely be gained by comparing the clear-sky fluxes only, since cloud forcing is not important to the study.*

Response

An important aspect of this study that needs to be noted is it is intended to provide season (one month) study of the radiative budget and sensitivities to water vapour and dust variability over the Saharan heat low. In order to do so we have used the best available input dataset through sensitivity experiments. It is useful to carry out comparison of the radiative flux at the time steps of CERES data (which is twice per day) as the referee suggested. We have actually made comparison of RT model outputs with CERES data with the respective time step to derive RMSE. This is presented on page 9 line 21(corrected draft). This will give us a good picture of the uncertainties of model simulations. However further comparisons using average of two time steps per day will not enable us to achieve the target we put at the outset.

To compare simulated flux with observation, GERB data is used. Further reanalysis data is also used which is available daily and thus used the same days as the RT model simulation days. CERES data is not used to compare simulated flux except for sensitivity experiments and estimate cloud DRE. We understand that using month mean CERES clear sky and all sky flux will bring some error but it will give us first order estimate of cloud DRE over the region. This will help emphasize need to improve the error on the radiative budget due to underestimated cloud in reanalysis dataset despite the challenges in making these comparisons.

5. *Flux comparisons: Tables and Figures. There are too many tables and the main figure (9) for this section is not particularly useful. Firstly, the tables are cumbersome and don't communicate the main results well (for example, color could be used to indicate if RT model output or reanalysis output is biased high or low in comparison to surface obs or satellite retrievals. In addition, the flux comparison Fig 9 are tough to interpret because the annual cycle is included. A better way to do this is to have one plot comparing the mean annual cycles, and another comparing the anomalies.*

Response

We agree to remove Table 5 since the information on this table is also found in Tables 2 and 3(corrected draft). An additional table is moved to the supplementary material.

Colours included on the wDwC results in tables 3 and 4(corrected draft Tables 2 and 3) red indicating model results overestimated and blue indicating model results underestimated compared with observation.

Some of the figures were corrected based on referee #1 and reviewer's comments. Figure 9(also Figure 6) is corrected and it is easier to read. We therefore keep it as it is. But have also made additional plot using anomalies but we put it in the supplementary document. See also page 9 L18-20.

Changes made

Table 5 removed
Colours used on column 6 of table 2 and table 3
Additional figure included in supplementary material page 3, figure S2

6. *Forcing efficiencies for dust and CIWV should also include the 95% confident interval from linear regressions.*

Response

We agree that the regressions should be expressed to 95% confidence level. All the regression results are expressed within the 95% confidence interval.

Changes made

These are included in section 4.2.1(page 10-11) and section 4.2.2(page 12) on the corrected draft.

7. *Figure 12 and 16 are not interesting. Consider including observations here as well (at least for TOA). BTW - CERES produces surface flux products. These could be folded into the analysis as well.*

Response

Here the plots are made using daily averaged variations in dust AOD or water vapour. That is dust AOD (and CIWV) is increased linearly in each RT run. This is a theoretical work designed to investigate the sensitivity of dust and water vapour on the radiation budget. There is no such observational data, at least at one particular point which is the observational data we used here. This

can be tested for a number of gridpoints of Satellite observation to see sensitivity of radiation to AOD variation (e.g Young et al., 2009). However this is not the objective of this study and thus it is not included.

8. *Figure 17 is impossible to read/interpret, and I don't even wear glasses (yet)! Please consider a more simple and straightforward way to describe the vertical sensitivities. A good rule-of-thumb would be to only include in the plot information that you actually describe in the text.*

Response

Figure made easier to read. Additional explanation regarding the figures provided

Changes made

Now we put the two panels of figure 17 as independent plots, Figure 16 and Figure 17 in the corrected draft.
Statement added on page 13, L18-19.

Minor Comments

1. *Individual panels of the figures should be labeled as a, b, c, ...*

Response

All figures prepared accordingly

2. *Figure 5: This figure is not very useful in terms of understanding the relationship between the AODs and IWV. Can you please just replace with one or two scatter plots?*

Response

We used SEVIRI AOD to show that there are cases where AOD is missed in AERONET which we suggest to be due to confusing dust with cloud. This we believe is important to show there are cases where dust might be missed in AERONET. We have complemented this using nephelometer measurements.

3. *Figure 6. If the authors removed the diurnal cycle from this plot we'd have an easier time interpreting the magnitude of the biases. As it is presented here, the magnitude of the differences are small relative to the magnitude of the diurnal temperature changes, making it difficult to interpret the results.*

Response

Figure 6 is now made easier to read and thus we keep it as it is. In addition we put the anomalies in the supplementary material. Additional information included in the supplementary material SP2 L:21-22

4. *Page 9, Line 2: You write "Dubovik Optical Properties" do you mean optical properties generated using the size distribution from Dubovik and the index of refraction that you've been using up to now (that hasn't been referenced)? It's just not clear.*

Response

Restated. Now on page 7 line 10 and 14.
Refractive index used comes from measurement. It is now made clear, Citation included, page 5 line 36

5. *Page 12, Paragraph starting on line 28: The finding that IWV and AOD contribute approximately equally to variance in the radiative budget is by far the most interesting (and new) finding reported in the paper. Why not take a little more space to flesh this out a bit? And please include the uncertainty estimates.*

Response

We agree this is an important point. Additional statement highlighting the significance of dust on controlling the radiative budget is included. Page 13 Line 4 of corrected draft.

Formatted: Indent: Before: 0 cm, First line: 0 cm

The Early summertime Saharan heat low: Sensitivity of the radiation budget and atmospheric heating to water vapor and dust aerosol.

Netsanet K. Alamirew[1*], Martin C. Todd[1*], C.L. Ryder[2], John H. Marsham[3], Y. Wang[1]

[1]Department of Geography, University of Sussex

[2]Department of Meteorology, University of Reading

[3]School of Earth and Environment, University of Leeds, UK

[*]Correspondence to: N. Alamirew na286@sussex.ac.uk or M. Todd m.todd@sussex.ac.uk

Abstract. The Saharan heat low (SHL) is a key component of the West African climate system and an important driver of the West African Monsoon across a range of timescales of variability. The physical mechanisms driving the variability in the SHL remain uncertain, although water vapour has been implicated as of primary importance. Here, we quantify the independent effects of variability in dust and water vapour on the radiation budget and atmospheric heating of the region using a radiative transfer model configured with observational input data from the Fennec field campaign at the location of Bordj Badji Mokhtar (BBM) in southern Algeria (0.9E, 21.4N), close to the SHL core, for June 2011. Overall, we find dust aerosol and water vapour to be of similar importance in driving variability in the top of atmosphere (TOA) radiation budget and therefore the column integrated heating over the SHL (~7 W m^{-2} per standard deviation of dust AOD). As such we infer that SHL intensity is likely to be similarly enhanced by the effects of dust and water vapour surge events. However, the details of the processes differ. Dust generates substantial radiative cooling at the surface (~11 W m^{-2} per standard deviation of dust AOD), presumably leading to reduced sensible heat flux into the boundary layer, which is more than compensated by direct radiative heating from SW absorption by dust in the dusty boundary layer. In contrast water vapour invokes a longwave radiative warming of at the surface of ~6 W m^{-2} per standard deviation of column integrated water vapour in Kg m^{-2}. Net effects involve a pronounced net atmospheric radiative convergence with heating rates on average of 0.5 K day^{-1} and up to 6 K day^{-1} during synoptic/meso-scale dust events from monsoon surges and convective cold pool outflows ('haboobs'). On this basis we make inferences on the processes driving variability in the SHL associated with radiative and advective heating/cooling. Depending on the synoptic context over the region processes driving variability involve both independent effects of water vapour and dust and compensating events in which dust and water vapour are co-varying. Forecast models typically have biases of up to 2 kg m^{-2} in column integrated water vapour (equivalent to a change in 2.6 W m^{-2} TOA net flux) and typically lack variability in dust, and so are expected to poorly represent these couplings. An improved representation dust and water vapour and quantification of associated radiative impact is thus imperative in quest for the answer to what remains to be uncertain related with the climate system of the SHL region.

1. Introduction

During boreal summer the Saharan Heat Low (SHL), a low-level thermal low, extends over a vast sector of the central Sahara Desert, covering much of northern Mauritania, Mali and Niger and Southern Algeria (Fig. ure 1). The area of low surface pressure is characterized by extremes of high surface temperature (Lavaysse

et al., 2009; Messager et al., 2010), and deep boundary layer (BL) ~~depth~~ (Marsham et al., 2013b), and is co-located with a global maximum in seasonal dust aerosol loading (Knippertz and Todd, 2012).

It is increasingly recognised that the SHL is a key component of the West African climate system and an important driver of the West African Monsoon across a range of timescales of variability e.g. (Chauvin et al., 2010; Couvreux et al., 2010; Lafore et al., 2010; Martin and Thorncroft, 2014; Martin et al., 2014; Parker et al., 2005; Peyrille and Lafore, 2007; Sultan and Janicot, 2003; Thorncroft and Blackburn, 1999; Xue et al., 2010). Notably, the intensification of the SHL in recent decades has been linked to the recovery of the Sahelian rainfall from the multi-decadal drought of the 1970s-90s, partly through a water vapour positive feedback process, in which radiative warming from increasing water vapour strengthens the SHL, which enhances the moist low level monsoon flow driving greater water vapour transport into the SHL and further warming (Dong and Sutton, 2015; Evan et al., 2015b; Lavaysse et al., 2016) with an implied enhanced West African Monsoon.

The SHL results from a complex interplay of heating processes within the Saharan BL, from the conversion of large radiative surpluses at the surface into sensible heat flux, cooling from horizontal temperature advection, itself a function of the strength of the pressure gradient into the SHL core, and radiative cooling and adiabatic warming via subsidence in the upper BL (Alamirew et al., submitted). The SHL intensity is therefore likely to be modulated by radiative effects of variability in surface albedo, dust aerosol, water vapour and cloud which feedback onto the circulation and thus advective cooling, water vapour transport and the processes governing dust emission and transport. In addition, the SHL is also modulated by external dynamical controls on advective cooling from both tropical (Knippertz and Todd, 2012) and extra-tropical sources (Chauvin et al., 2010).

Previous studies have quantified direct radiative effects (DRE) of dust aerosol at the top of atmosphere (TOA) and surface from in situ observations and satellite data (Ansell et al., 2014; Banks and Brindley, 2013; Yang et al., 2009), whilst Marsham et al., 2016, hereafter M16, extend this empirically to consider water vapour variations, and implicitly cloud, as well as dust. However, there remain important gaps in our understanding. First, there are substantial uncertainties in the magnitudes of radiative fluxes (and other heat budget terms) across both the various reanalyses and observations. Second, separating the radiative effects of water vapour ~~from both~~ from both its and associated clouds and from dust aerosol is challenging from observations, given the strong co-variability of dust and total column water vapour (TCWV) anomalies in the Sahara associated with monsoon surges and resulting convective cold pool events ('haboobs') which transport water vapour and dust into the central Sahara (Garcia-Carreras et al., 2013; Marsham et al., 2008; Marsham et al., 2013b). As such, there is a need to quantify more fully the DRE of dust and water vapour, both independently and together, over the Sahara. This information is necessary to resolve the processes that govern the fundamental structure and maintenance and variability of the SHL. Addressing these research gaps is hindered by the acute shortage of routine observations in the region and large discrepancies between models and reanalyses (Evan et al., 2015a; Roberts et al., 2015).

This paper seeks to address these gaps in our understanding of radiative processes within the SHL during early summer. Specifically, to quantify the separate roles of water vapour and dust aerosol in controlling the top of atmosphere, surface, and the vertical profile of the atmospheric column radiative budget. This will be achieved through radiative transfer (RT) model simulations using uniquely detailed observations of atmospheric conditions over the SHL region during early summer, including those from the main supersite of the recent

Fennec field campaign (Marsham et al., 2013b). Best estimates and associated uncertainty are established through a set of RT model experiments testing the sensitivity of radiative flux and atmospheric heating rates to ~~variability in~~ water vapour and dust variability and to uncertainty in a set of controlling variables. In this way, we can inform interpretation of hypotheses on drivers of SHL variability and its wider impact on the regional climate. A description of the radiative transfer code is given in section 2 followed by list of input data used to run the RT model in section 3. The different experiments used towards the optimal model configuration are presented in section 4. Results of the mean state and sensitivity RT runs for water vapour and dust are given in section 4. The paper is concluded by presenting the summary and conclusion of our results in section 5.

2. Description of the SOCRATES Radiative Transfer model ~~and observed radiative flux data~~

~~2.1 The SOCRATES Radiative Transfer model~~

The research questions are addressed through simulations from a column stand-alone RT model. Such models are commonly used for detailing the combined and unique radiative impact of dust aerosol and water vapour (Osborne et al., 2011; Osipov et al., 2015; Otto et al., 2007; Otto et al., 2009; Otto et al., 2011; Slingo et al., 2006). RT models typically comprise a radiative transfer core and a pre-processor to configure the necessary information on the radiatively active atmospheric constituents and surface characteristics. Typically, these include meteorological and gas component profiles ~~from observations, reanalysis products or weather/climate models~~, ~~spectral~~ aerosol optical properties and~~y~~ profiles, and surface optical properties.

Here we use ~~the~~ SOCRATES (Suite Of Community Radiative Transfer codes based on Edwards and Slingo) (Edwards and Slingo, 1996; Randles et al., 2013) model configured with observed and idealised profiles of water vapour and dust aerosol, as described below. SOCRATES is a flexible RT model, operated here in two streams of standalone radiative transfer code, which calculates the longwave and shortwave radiative fluxes and heating rates throughout the atmosphere given the atmospheric and surface properties of that column, the solar zenith for the location, date and time. Radiative flux calculations are made for parallel plane atmosphere with spectral resolution ranging over the ~~shortwave and~~shortwave and longwave from 0.2 to 10 μm divided in 6 bands and 3.3 μm to 10,000 μm~~,~~ divided in~~n 6 and~~ 9 bands respectively. Column atmospheric and surface characteristics are required to run the RT model which are described in sections 3.2 and section 3.3. A detailed description of the model is given in (Randles et al., 2013).

Formatted: Indent: First line: 1.27 cm

3. Data and Methods

3.1. Observed top of atmosphere and surface radiation measurements

~~Inputs for the model are meteorological fields (temperature, specific humidity), active radiative gases (O_2, CO_2, CH_4, CO, N_2O, and O_3), surface fields (skin temperature, surface pressure, broadband albedo, and emissivity), dust aerosol optical properties and the vertical profile of dust mass mixing ratio. A detailed description of the model is given in (Randles et al., 2013).~~

We use satellite retrievals of TOA radiation from two sources. 1). The EUMETSAT Geostationary Earth Radiation Budget (GERB) (Harries et al., 2005) level 2 products of Averaged Rectified Geolocated (ARG) fluxes at approximately 17 minute time and 50km spatial (at nadir) resolution, with spectral ranges 0.32 to 4μm in the shortwave and 4 to 100 μm in the longwave. 2). The Clouds and the Earth's Radiant energy System (CERES) (Wielicki, 1996) instrument which has channels that measure total radiance (0.4-200μm) and shortwave radiance (0.4-4.5μm). Since there is no longwave-only channel on CERES, daytime longwave radiances are determined from the difference between the total and shortwave channel radiances. We use two CERES products: (i) the monthly mean Energy Balanced and Filled (EBAF) product at 1-degree resolution. (ii) The CERES Level-3 SSF1deg Hour TERRA footprint gridded data (CERES-footprint) instantaneous, twice daily with 1-degree resolution.

For our high resolution, pixel based analysis focused on a single location (BBM), cloud screening is notoriously challenging. For GERB data we apply the EUMETSAT cloud mask to derive clear sky and all-sky conditions and for CERES data we use both all sky and clear sky products. MODIS cloud parameters are used to derive CERES cloud free fluxes. However, analysis of GERB all-sky minus clear-sky fluxes at BBM suggests ~~an~~ unrealistically small cloud DRE (~2 $W.m^{-2}$ in longwave flux), which indicate~~suggest~~s that the cloud mask is not robust. We therefore choose only to use GERB all sky fluxes and limit the clear sky-only analysis to the CERES products. For 'validation' of the 'optimum' model configuration (see section 4), we favour comparison with GERB (all-sky) because the time period of the CERES monthly product is not exactly compatible with the RT simulations of 8th-30th June, whilst the CERES footprint data has observations twice daily.

Surface measurements of shortwave and longwave upwelling and downwelling radiation are obtained from Kipp and Zonen CNR4 radiometers situated at 2m height deployed at BBM during the FENNEC campaign (Marsham et al., 2013b).

3.2 Atmospheric profile and surface characteristics

Input data which are required to run the RT model for the model are meteorological fields (temperature, specific humidity), cloud mixing ratio and fraction, active radiative gases vertical profile mixing ratios, surface optical properties (skin temperature, surface pressure, broadband albedo, and emissivity). To include the effect of aerosols in RT simulations, optical properties and the vertical profile mass mixing ratio of the desired aerosol should be provided. ~~We also use the skin temperature product form CERES Level 3 SSF1deg Hour TERRA footprint data.~~

We specify these inputs as accurately as possible using observations from the recent Fennec field campaign, which obtained unique data from within the SHL region during June 2011 (Ryder et al., 2015). We use observations from ground-based instruments deployed at the~~the main~~ Fennec supersite at ~~Bordji Badji Mokthar (~~BBM~~) 0.9E, 21.4N and 420m elevation close to the Aljeria-Mali border~~ (Marsham et al., 2013b) and various aircraft flights (see Ryder et al., 2015 for overview) complemented~~, where direct observations are inadequate,~~ with fields from the European Centre for Medium-Range Weather Forecasts (ECMWF) Interim Reanalysis (ERA-I) (Dee et al., 2011) and Modern-Era Retrospective analysis for Research and Application (MERRA) (Rienecker et al., 2011) reanalysis, where direct observations are inadequate.~~.~~

Formatted: Indent: First line: 1.27 cm

Formatted: Superscript

Formatted: Indent: First line: 1.27 cm

Formatted: Font: (Default) +Headings CS (Times New Roman), 10 pt, Complex Script Font: +Headings CS (Times New Roman), 10 pt

Profiles of temperature and water vapour (Fig. 2) are obtained from radiosonde measurements at BBM for June 8th-30th, 2011 ~~(Figure 2)~~. The temporal resolution of radiosonde measurements varied from 3-6 hour~~ly~~ over the study period. A distinction can be made between the cooler, drier, less dusty Saharan 'maritime' phase from around 8th to 12th June to a hotter, moister, dustier 'heat low' phase from around 13th to 30th June (Fig. 2a) during which time both synoptic scale monsoon surges and meso-scale convective cold pool events transported both water vapour and dust into the heart of the SHL (see Ryder et al., 2015; Todd et al., 2013 for full details). For comparison, profiles of water vapour from Era-I reanalysis are shown in Fig. 2b. Despite the good agreement between measurement and model outputs, ERA-I underestimates specific humidity in the lowest level by ~4.9% (MERRA by 5.5%). The possible reasons for the remaining error between observation and reanalysis products could be due to differences in models core dynamics and assimilation procedures. Note that the error in reanalysis at BBM is relatively small because the Fennec radiosondes data were assimilated. In the subsequent absence of such observational data we expect reanalysis errors to be greater given the known problems of reanalysis model representation of meso-scale convective processes in the region (Garcia-Carreras et al., 2013; Roberts et al., 2015; Todd et al., 2013). Such mesoscale convective 'cold pool' outflows (known locally as 'haboobs') are known to make a significant contribution to moisture advection as well as being the dominant dust emission process (Marsham et al., 2013b; Trzeciak et al., 2017). Red arrows in Fig. 2a denote major haboob events.

Profiles of trace gases required for ~~needed by~~ the radiative transfer model (CO_2, O_2, N_2O, O_3, and CH_4) are taken from the standard tropical atmosphere (Anderson et al., 1986). Temperature and water vapour profiles beyond the upper maximum height of the radiosonde data (approximately 20 km) are also taken from the standard tropical atmosphere. This is unlikely to affect RT model results significantly since there is little day to day variability in the uppermost part of the atmosphere. ~~A distinction can be made between the cooler, drier, less dusty Saharan 'maritime' phase from around 8th to 12th June to a hotter, moister, dustier 'heat low' phase from around 13th to 30th June (Figure 2a) during which time both synoptic scale monsoon surges and meso-scale convective cold pool events transported both water vapour and dust into the heart of the SHL (see Ryder et al., 2015; Todd et al., 2013 for full details).~~

Acquiring observations of the vertical structure of clouds of sufficient quality for radiative transfer calculations is always challenging. Here we use the ERA-I and MERRA outputs of cloud fraction, liquid and ice water mixing ratios. Cloud is treated to have maximum overlap in a column where ice and water are mixed homogeneously. During the Fennec period, cloud was characterised by shallow cumulus or altocumulus near the top of the PBL and occasional deep convection. It is likely that the relatively coarse vertical and horizontal resolution of both reanalysis models will have considerable bias and we recognise that this is likely to underestimate the true cloud-related uncertainty, and for example, M16 suggest that ERA-I underestimate cloud fraction by a factor of 2.5.

We calculate surface albedo from surface observations of shortwave flux at BBM for the days when good measurement is available (see Fig. 3). During the days where measurements were not good, we use the diurnal average surface albedo of all other days. The mean surface albedo at BBM is 0.36 and shows strong diurnal cycle, varying with solar zenith angle giving maximum surface shortwave reflection during the morning and evening hours, i.e. when the sun is at high solar zenith angles. This has an impact on the diurnal cycle of dust radiative effect (Ansell et al., 2014;Banks et al., 2014;Osipov et al., 2015). Fennec does not provide

Formatted: Indent: First line: 1.27 cm

measurements of skin temperature and thus we look for alternative best approximates from ERA-I and MERRA. For comparison, we also use the skin temperature product form CERES Level-3 SSF1deg Hour TERRA footprint data. Figure 4 shows time series of skin temperature and 2 m air temperature from observation and reanalysis.

3.3. Dust optical properties and extinction profile

Dust radiative effect is known to be influenced by size distribution (Otto et al., 2009; Ryder et al., 2013a, b), which remains uncertain over the Sahara. We test the RT model sensitivity to two different and highly contrasting dust size distributions: (i) derived using AERONET sun photometer inversions from Cape Verde, representative of transported dust (Dubovik et al., 2002), referred to as Dubovik hereafter and (ii) measured directly from aircraft observations during the Fennec campaign (Ryder et al., 2013b) referred to as Fennec-Ryder hereafter, which include a pronounced coarse-mode with effective diameter in the range between 2.3 and 19.4 μm, contrasting with the much finer size distribution of Dubovik from AERONET. In both cases the dust size distributions and same measured refractive index (Ryder et al., 2013b) are used as inputs to Mie code in the RT pre-processor from which the optical properties of dust are calculated, specifically the single scattering albedo (ω or SSA), mass extinction coefficient (known as MEC or K_{ext} units $m^2 Kg^{-1}$), and asymmetry parameter (g), for the relevant spectral bands applied in the RT model. Figure 5 displays the wavelength dependence of optical properties for both Dubovik and Fennec-Ryder dust size distributions. The continuous lines are the spectrally resolved optical properties and the horizontal lines are the band-averaged data which are used in the RT code. Further information on the optical properties for the two dust distributions is provided in the supplementary material (section S1).

No observations of the vertical profile of dust loading at BBM are available from the Fennec instrumentation. Since the model requires the vertical distribution of mass mixing ratio of dust as an input, we use the long term mean extinction coefficient profiles for dust aerosol derived from the Cloud-Aerosol Lidar with Orthogonal Polarization (CALIOP) (Liu et al., 2009; Winker et al., 2009) satellite instrument. Data from all individual CALIOP satellite orbits over the 2006-14 period were quality controlled and screened to retain dust aerosol only observations using the method described in Todd and Cavazos-Guerra (2016), which provides sampling for robust characterisation of aerosol distribution in 3 dimensions (Ridley et al., 2012; Todd and Cavazos-Guerra, 2016; Winker et al., 2009). The long term mean extinction coefficient profile at BBM (Fig. 6) shows a regular decrease of extinction through the aerosol layer which extends up to about 5 km at the top of the planetary boundary layer, which is also seen in Fennec airborne measurements from 2011 (Ryder et al., 2013a). This extinction profile is scaled at each model time step to yield the observed column integrated AOD from the BBM AERONET sunphotometer. We then use the mass extinction coefficient (in $m^2 Kg^{-1}$) to convert dust extinction coefficient (in m^{-1}) to dust mass mixing ratio (kg/kg) as required by the model (e.g. Greed et al., 2008). Mass extinction coefficient is calculated from Mie code (see Fig. 5).

AOD data used to scale the mean extinction coefficient profiles are taken from retrievals form the AErosol RObotic NETwork (AERONET) (Holben et al., 1998) instrument at BBM, using Level-2 data, which is cloud screened and quality assured. We compared AERONET AOD with estimates of AOD from the SEVIRI instrument on Meteosat 9 satellite (derived from the 550nm channel using the algorithm of Banks and Brindley

Formatted: Indent: First line: 1.27 cm

(2013)) over the June 2011 study period (Fig. 7). The more frequent dust events during the latter half of the month (heat low phase) compared to the earlier heat maritime phase is apparent, with dust events frequently associated with high water vapour indicative of convective cold pool 'haboob' dust events (see Fig. 2a). The estimates of mean AOD agree to within 20% and there is a strong correlation between the two estimates of 0.7, despite some apparent dust events apparent in SEVIRI but not AERONET e.g. 13th and 29th June. This is mainly due to AERONET masking dust as cloud particularly in cases when dust and cloud coexist.

Nigh time dust emission is common during summer in the SHL region, although we expect dust shortwave daytime radiative effect to be dominant (Banks et al., 2014). Estimation of AOD at night is problematic for most passive instruments and we use the following method: estimate AOD from observations of scattering from the nephelometer instrument deployed near the surface at BBM (Rocha-Lima et al., submitted), based on the regression of scattering to column integrated AOD during coincident daytime observations. The nephelometer-based estimates of AOD will account for night time emission of dust due to Haboobs (Marsham et al., 2013) but since haboobs tend to occupy a shallow layer, than the better mixed daytime dust, this will tend to overestimate AODs estimated at night. However this will not bring significant effect on the overall result since at night there
is only longwave forcing which is small compared with shortwave forcing.

Formatted: Indent: First line: 0 cm

3.4. RT model experiments

Formatted: Indent: First line: 1.27 cm

~~For comparison, profiles of water vapour from radiosonde measurements with Era-I reanalysis are shown in Figure 2b. Despite the good agreement between measurement and model outputs, ERA-I underestimates specific humidity in the lowest level by ~4.9% (MERRA by 5.5%). Note that the error in reanalysis at BBM is relatively small because the Fennec radiosondes data were assimilated. In the subsequent absence of such observational data we expect reanalysis errors to be greater given the known problems of reanalysis model representation of meso-scale convective processes in the region (Garcia-Carreras et al., 2013; Roberts et al., 2015; Todd et al., 2013). Such mesoscale convective 'cold pool' outflows (known locally as 'haboobs') are known to make a significant contribution to moisture advection as well as being the dominant dust emission process (Marsham et al., 2013b; Trzeciak et al., 2017). Red arrows in Figure 2a denote major haboob events.~~

We undertake two types of RT experiment in this study:

Formatted: Indent: First line: 0 cm

(i) **M~~m~~odel 'configuration mode'** through~~in~~ which we test the sensitivity of simulated radiative fluxes to uncertainty in as many of the input variables as possible (see supplementary material Section S2~~, as described in Section 3.2, summarised in Table 1)~~. The description and results of all sensitivity experiments to choice of different input data are provided in the supplementary material (Section S3 and Table S1). Here we present the results of the sensitivity experiments to dust size distribution since it is an important part of the paper. Sensitivity to the two contrasting dust size distributions is pronounced. As expected results using Fennec-Ryder dust show much stronger absorption in the shortwave compared with the Dubovik dust distribution, and the resulting TOA net shortwave flux is higher by 25 W m^{-2} in the former. These shortwave fluxes using Fennec-Ryder distribution are not consistent with the GERB/CERES satellite observations (nor with previous estimates of shortwave DRE derived from satellite e.g. Yang et al. (2009); Ansell et al. (2014)) and we use dust optical properties generated using Dubovik size distribution in the optimum configuration. Recent work

Formatted: Font: Bold

suggests that the dust optical properties at BBM in June 2011 were significantly less absorbing than both those measured by the aircraft further west during Fennec, and the Dubovik representation (less absorbing, smaller sized) with SSA values of 0.99 (Rocha-Lima et al., submitted). Therefore, optical properties generated using Dubovik size distribution and measured refractive index represent intermediate values in terms of SW absorption.

Given that we don't have accurate data for all the input required to run the RT model, it is not unexpected to get some uncertainty in our results. However we have chosen the inputs in such a way that the calculated flux are as close as possible to observation. This will result in an acceptably configured model for experimental analysis presented next.

(ii) Model 'experiment mode' through which ~~Using the suitably configured RT model (from Section 4.1)~~ we addressed the research questions, specifically to quantify the combined and separate DRE of water vapour and dust. To this end~~,~~ we undertook a number of experiments summarized in Table 1~~2~~, with results described in Section 4~~i.e. the 'experiment mode'~~. For all the experiments, RT calculations are made for each day using the atmospheric profiles at hourly time steps over the diurnal cycle, and the mean flux and heating rates are derived by averaging outputs at each time step. For this purpose, ~~A~~all input data are linearly interpolated to a one-hour temporal resolution.

For experiments with ('w') and without ('n') dust ('D') we simulate the 8th-30th June 2011 period. For sensitivity ('sen') experiments, we simulate linearly increased levels of dust AOD and water vapour. We use runs both with cloud ('C') and with no cloud (nC). For dust sensitivity experiment ('senDnC'), AOD is increased linearly over the range 0 (dust free) to 3 (extremely dusty), while keeping the mean value of water vapour constant. For water vapour sensitivity experiment ('senWVwDnC') the mean diurnal profile of water vapour is used but is scaled so that the column integrated water vapour increases from 10 to 40 kg m^{-2} and the mean AOD is used in each case. The DRE for dust is derived by (i) subtracting TOA and surface fluxes of experiment wDnC from nDnC (ii) linear regression of the flux dependence on the range of dust AOD from the dust sensitivity experiments (senDnC), in which a single diurnal cycle is simulated. The impact of water vapour is determined by (i) composites of dry versus humid days from the nDnC experiment (ii) linear regression of the flux dependence on the range of water vapour from water vapour sensitivity experiments (senWVwDnC). The results of DRE of dust and water vapour are presented in Section 4.2.

~~with results provided in Section 4.1. This will result in an acceptably configured model for experimental analysis. (ii) Model 'experiment mode' to specifically address the research questions using the 'optimal' model configuration. The experiments are described in Section 3.3, summarised in Table 2, with results described in Section 4.2. These include RT model experiments run for durations from one day to one month (June 2011).~~

~~**2.2 Observed top of atmosphere and surface radiation measurements for comparison with RT simulations**~~

~~We use satellite retrievals of TOA radiation from two sources. 1). The EUMETSAT Geostationary Earth Radiation Budget (GERB) (Harries et al., 2005) level 2 products of Averaged Rectified Geolocated (ARG) fluxes at approximately 17 minute time and 50km spatial (at nadir) resolution, with spectral ranges 0.32-~~

Formatted: Indent: First line: 1.27 cm

to 4μm in the shortwave and 4 to 100 μm in the longwave. 2). The Clouds and the Earth's Radiant energy System (CERES) (Wielicki, 1996) instrument which has channels that measure total radiance (0.4-200μm) and shortwave radiance (0.4-4.5μm). Since there is no longwave-only channel on CERES, daytime longwave radiances are determined from the difference between the total and shortwave channel radiances. We use two CERES products: (i) the monthly mean Energy Balanced and Filled (EBAF) product at 1-degree resolution. (ii) The CERES Level-3 SSF1deg_Hour TERRA footprint gridded data (CERES footprint) instantaneous, twice daily with 1-degree resolution.

For our high resolution, pixel based analysis focused on a single location (BBM), cloud screening is notoriously challenging. For GERB data we apply the EUMETSAT cloud mask to derive clear-sky and all-sky conditions and for CERES data we use both all-sky and clear-sky products. MODIS cloud parameters are used to derive CERES cloud free fluxes. However, analysis of GERB all-sky minus clear-sky fluxes at BBM suggests an unrealistically small cloud DRE (~2 $W.m^{-2}$ in longwave flux), which suggests that the cloud mask is not robust. We therefore choose only to use GERB all-sky fluxes and limit the clear-sky only analysis to the CERES products. For 'validation' of the 'optimum' model configuration, we favour comparison with GERB (all-sky) because the time period of the CERES monthly product is not exactly compatible with the RT simulations of 8-20th June, whilst the CERES footprint data has observations twice daily.

Surface measurements of shortwave and longwave upwelling and downwelling radiation are obtained from Kipp and Zonen CNR4 radiometers situated at 2m height deployed at BBM during the FENNEC campaign (Marsham et al., 2013b). We also use the skin temperature product form CERES Level-3 SSF1deg_Hour TERRA footprint data.

3 Description of RT model experiments and input data

3.1. Input data common to all experiments

3.1.1 Atmospheric data

Profiles of temperature and water vapour are obtained from radiosonde measurements at BBM for June 8th-30th 2011 (Figure 2). The temporal resolution varied from 3-6 hourly over the study period. Profiles of trace gases needed by the radiative transfer model (CO_2, O_3, N_2O, O_2, and CH_4) are taken from the standard tropical atmosphere (Anderson et al., 1986). Temperature and water vapour profiles beyond the upper maximum height of the radiosonde data (approximately 20 km) are also taken from the standard tropical atmosphere. This is unlikely to affect RT model results significantly since there is little day-to-day variability in the uppermost part of the atmosphere. A distinction can be made between the cooler, drier, less dusty Saharan 'maritime' phase from around 8th to 12th June to a hotter, moister, dustier 'heat-low' phase from around 13th to 30th June (Figure 2a) during which time both synoptic scale monsoon surges and meso-scale convective cold pool events transported both water vapour and dust into the heart of the SHL (see Ryder et al., 2015; Todd et al., 2013 for full details). For comparison, profiles of water vapour from radiosonde measurements with Era-I reanalysis are shown in Figure 2b. Despite the good agreement between measurement and model outputs, ERA-I underestimates specific humidity in the lowest level by ~4.9% (MERRA by 5.5%). Note that the error in

reanalysis at BBM is relatively small because the Fennec radiosondes data were assimilated. In the subsequent absence of such observational data we expect reanalysis errors to be greater given the known problems of reanalysis model representation of meso-scale convective processes in the region (Garcia-Carreras et al., 2013; Roberts et al., 2015; Todd et al., 2013). Such mesoscale convective 'cold pool' outflows (known locally as 'haboobs') are known to make a significant contribution to moisture advection as well as being the dominant dust emission process (Marsham et al., 2013b; Trzeciak et al., 2017). Red arrows in Figure 2a denote major haboob events.

3.1.2 Surface albedo

We calculate surface albedo from surface observations of shortwave flux at BBM for the days when good measurement is available (see Figure 3). During the days where measurements were not good, we use the diurnal average surface albedo of all other days. The mean surface albedo at BBM is 0.36 and shows strong diurnal cycle, varying with solar zenith angle giving maximum surface shortwave reflection during the morning and evening hours, i.e. when the sun is at high solar zenith angles. This has an impact on the diurnal cycle of dust radiative effect (Ansell et al., 2014;Banks et al., 2014;Osipov et al., 2015).

3.1.3. Dust AOD

No observations of the vertical profile of dust loading at BBM are available from the Fennec instrumentation. Since the model requires the vertical distribution of mass mixing ratio of dust as an input, we use the long term mean extinction coefficient profiles for dust aerosol derived from the Cloud-Aerosol Lidar with Orthogonal Polarization (CALIOP) (Liu et al., 2009; Winker et al., 2009) satellite instrument. These are then scaled at each model time step to yield the observed column integrated AOD from the BBM AERONET sunphotometer. We then use the mass extinction coefficient (in $m^2 Kg^{-1}$) to convert dust extinction coefficient (in m^{-1}) to dust mass mixing ratio (kg/kg) as required by the model (e.g. Greed et al., 2008). Mass extinction coefficient is calculated from Mie code (see Figure 7). Data from all individual CALIOP satellite orbits over the 2006-14 period were quality controlled and screened to retain dust aerosol only observations using the method described in Todd and Cavazos-Guerra (2016), which provides sampling for robust characterisation of aerosol distribution in 3 dimensions (Ridley et al., 2012; Todd and Cavazos-Guerra, 2016; Winker et al., 2009). The long term mean extinction coefficient profile at BBM (Figure 4) shows a regular decrease of extinction through the aerosol layer which extends up to about 5 km at the top of the planetary boundary layer, which is also seen in Fennec airborne measurements from 2011 (Ryder et al., 2013a).

AOD data used to scale the mean extinction coefficient profiles are taken from retrievals form the AErosol RObotic NETwork (AERONET) (Holben et al., 1998) instrument at BBM, using Level-2 data, which is cloud screened and quality assured. We compared AERONET AOD with estimates of AOD from the SEVIRI instrument on Meteosat 9 satellite (derived from the 550nm channel using the algorithm of Banks and Brindley (2013)) over the June 2011 study period (Figure 5). The more frequent dust events during the latter half of the month (heat low phase) compared to the earlier heat maritime phase is apparent, with dust events frequently associated with high water vapour indicative of convective cold pool 'haboob' dust events (see Figure 2a). The

estimates of mean AOD agree to within 20% and there is a strong correlation between the two estimates of 0.7, despite some apparent dust events apparent in SEVIRI but not AERONET e.g. 13th and 29th June. This is mainly due to AERONET masking dust as cloud particularly in cases when dust and cloud coexist.

Nigh time dust emission is common during summer in the SHL region, although we expect dust shortwave daytime radiative effect to be dominant (Banks et al., 2014). Estimation of AOD at night is problematic for most passive instruments and we use the following method: estimate AOD from observations of scattering from the nephelometer instrument deployed near the surface at BBM (Rocha-Lima et al., submitted), based on the regression of scattering to column integrated AOD during coincident daytime observations. The nephelometer-based estimates of AOD will account for night time emission of dust due to Haboobs (Marsham et al., 2013) but since haboobs tend to occupy a shallow layer, than the better mixed daytime dust, this will tend to overestimate AODs estimated at night.

3.2 RT configuration mode experiments towards 'optimal' configuration

For some quantities, we do not have direct observations so we use alternative data from various sources. In the 'configuration mode' we test the uncertainty of the modelled radiative fluxes to uncertainties in these model inputs using the experiments summarised in Table 1. Then comparison of TOA fluxes with satellite observation allows us to arrive at what we consider to be an 'optimal' model configuration for the subsequent model 'experiment mode' analysis.

3.2.1 Surface condition data

Fennec does not provide observations of all the necessary information for the RT model and thus we look for alternative best approximates from ERA-I and MERRA data of the following quantities:

(i) Surface skin temperature. Since there are no complete observations of skin temperature we use reanalysis products as inputs to the RT code and we use both these data to further investigate sensitivity of flux to uncertainty in skin temperature. Figure 6 displays the time series of surface skin temperature from ERA-I, MERRA, and CERES footprint data. Root mean square error (RMSE) of the reanalysis products with respect to CERES footprint data are high (4.5 K and 5.5 K for MERRA and ERA-I, respectively). Despite the higher RMSE of ERA-I skin temperature compared with RMSE of MERRA, the RMSE of ERA-I 2 m air temperature (Figure 6) with respect to flux tower measurement is 3.1 K (3.7 K, MERRA). The relatively bigger RMSE in skin temperature could be due to the uncertainty in CERES measurements.

(ii) Surface emissivity. We test the sensitivity of radiative fluxes to uncertainty in estimates of surface emissivity using CERES measurements (mean=0.89) and MERRA outputs (mean =0.94).

(iii) Surface albedo. We noted that in contrast to observations the reanalysis products have weak representation of the diurnal cycle in surface albedo (Figure 3). Although we use observed surface albedo throughout all our experiment model RT runs, we also test the sensitivity of TOA shortwave flux to reanalysis surface albedo errors.

3.2.2 Dust size distribution

Dust radiative effect is known to be influenced by size distribution (Otto et al., 2009; Ryder et al., 2013a, b), which remains uncertain over the Sahara. We test the RT model sensitivity to two different and highly contrasting dust size distributions: (i) derived using AERONET sun photometer inversions from Cape Verde , representative of transported (Dubovik et al., 2002), referred to as Dubovik hereafter and (ii) measured directly from aircraft observations during the Fennec campaign (Ryder et al., 2013b) referred to as Fennec-Ryder hereafter, which include a pronounced coarse-mode with effective diameter in the range between 2.3 and 19.4 μm, contrasting with the much finer size distribution of Dubovik from AERONET. In both cases the dust size distributions and the same refractive index are used as inputs to Mie code in the RT pre-processor from which the optical properties of dust are calculated, specifically the single scattering albedo (ω or SSA), mass extinction coefficient (known as MEC or K_{ext} units $m^2 Kg^{-1}$), and asymmetry parameter (g), for the relevant spectral bands applied in the RT model. Figure 7 displays the wavelength dependence of optical properties for both Dubovik and Fennec-Ryder dust size distributions. The continuous lines are the spectrally resolved optical properties and the horizontal lines are the band-averaged data which are used in the RT code. SSA values in the band covering the spectral range 0.32 to 0.69 μm are 0.82 and 0.91 for Fennec-Ryder and Dubovik respectively. The coarser particles in Fennec Ryder result in a lower SSA – i.e. more absorbing dust. Note that in the model since the AOD is fixed based on the observed AOD, the vertical profile of dust mass mixing ratio is adjusted so that when combined with the MEC shown in Figure 7, the AOD in the spectral range 0.32 to 0.69 μm is correct. Therefore the differences in MEC between the two datasets shown in Figure 7 are cannot result in differences within the RT model. However, differences in SSA and g are able to exert different impacts on the radiative fluxes within the RT model, as described in section 4.1

3.2.3 Cloud properties

Acquiring observations of the vertical structure of clouds of sufficient quality for radiative transfer calculations is always challenging. Here we use the ERA-I and MERRA outputs of cloud fraction, liquid and ice water mixing ratios. Cloud is treated to have maximum overlap in a column where ice and water are mixed homogeneously. During the Fennec period, cloud was characterised by shallow cumulus or altocumulus near the top of the PBL and occasional deep convection. It is likely that the relatively coarse vertical and horizontal resolution of both reanalysis models will have considerable bias and we recognise that this is likely to underestimate the true cloud-related uncertainty, and for example, M16 suggest that ERA-I underestimate cloud fraction by a factor of 2.5.

3.3 RT model 'experiment mode' design

Using the suitably configured RT model (from Section 4.1) we addressed the research questions, specifically to quantify the combined and separate DRE of water vapour and dust, we undertook a number of experiments summarized in Table 2, i.e. the 'experiment mode'. For all the experiments RT calculations are made for each day using the atmospheric profiles at hourly time steps over the diurnal cycle, and the mean flux

~~and heating rates are derived by averaging outputs at each time step. All input data are linearly interpolated to a one-hour temporal resolution.~~

~~For the experiments with ('w') and without ('n') dust ('D') we simulate the 8th-30th June 2011 period. For the sensitivity ('sen') experiments, we simulate linearly increased levels of dust AOD and water vapour. We use runs both with cloud ('C') and with no cloud (nC). For dust sensitivity experiment ('senDnC'), AOD is increased linearly over the range 0 (dust free) to 3 (extremely dusty), while keeping the mean value of water vapour constant. For water vapour sensitivity experiment ('senWVwDnC') the mean diurnal profile of water vapour is used but is scaled so that the column integrated water vapour increases from 10 to 40 kg m^{-2} and the mean AOD is used in each case.~~

~~The DRE for dust is derived by (i) subtracting TOA and surface fluxes of experiment wDnC from nDnC (ii) linear regression of the flux dependence on the range of dust AOD from the dust sensitivity experiments (senDnC), in which a single diurnal cycle is simulated. The results are presented in Section 4.2. The impact of water vapour is determined by (i) composites of dry versus humid days from the nDnC experiment (ii) linear regression of the flux dependence on the range of water vapour from the water vapour sensitivity experiments (senWVwDnC).~~

4. Results and discussion

4.1. RT model ~~RT model~~ validation ~~optimum configuration and validation~~

Prior to testing the main research questions related to the relative roles of dust and water vapour in radiative heating ~~(Section 4.2)~~, the RT model was configured based on the 'configuration mode' sensitivity analyses (described in supplementary material, section S2~~in Section 3.1, Table 1~~) and comparison with observed TOA fluxes from the CERES-EBFA monthly mean product (clear sky in the case of all sensitivity analysis except the cloud sensitivity which we compare to CERES-EBFA all sky). The results of sensitivity experiments for the various input parameters are presented in supplementary document of this paper (section S3) and list of selected input parameters for further experiments are shown in table S1 (column 4).

~~Sensitivity of RT simulated fluxes to uncertainty in the surface skin temperature and emissivity is low compared to the sensitivity to other factors (Table 1) with variations of ~2 W m^{-2} at TOA and 5-6 W m^{-2} at surface. Based on bias with respect to CERES-EBFA observations we use ERA-I skin temperature and MERRA emissivity products for the 'optimal' configuration.~~

~~Sensitivity to the two contrasting dust size distributions is pronounced. As expected results using Fennec-Ryder dust show much stronger absorption in the shortwave compared with the Dubovik dust distribution, and the resulting TOA net shortwave flux is higher by 25 W m^{-2} in the former. These shortwave fluxes using Fennec-Ryder are not consistent with the GERB/CERES satellite observations (nor with previous estimates of shortwave DRE derived from satellite e.g. Yang et al. (2009); Ansell et al. (2014)) and we use Dubovik optical properties in the optimum configuration. Recent work suggests that the dust optical properties at BBM in June 2011 were significantly less absorbing than both those measured by the aircraft further west during Fennec, and the Dubovik representation (less absorbing, smaller sized) with SSA values of 0.99 (Rocha-~~

Formatted: Indent: First line: 1.27 cm

~~Lima et al., submitted). Therefore, Dubovik optical properties represent intermediate values in terms of SW absorption.~~

~~TOA fluxes are not strongly sensitive to the choice of cloud properties with TOA net flux variations of ~4 W m^{-2}. On the basis of bias with respect to observations we select the ERA-I cloud properties. It is interesting to note that TOA radiative fluxes are quite sensitive to the errors in surface albedo from reanalysis with differences up to 16 W m^{-2} compared to the optimum configuration, which used observed surface albedo. This suggests that it is important to have good observational data, which captures the strong diurnal cycle of surface albedo to achieve accurate radiative fluxes.~~

The RT model with the above choices of input data is considered to be the 'optimum' configuration, and we validate TOA and surface fluxes with respect to satellite and surface observations, respectively (Tables 2~~3~~ and 3~~4~~) for the most 'realistic' experiment wDwC. The sign convention used here and in the remainder of the paper is that downward flux is considered as positive while upward radiation is negative.

The simulated TOA net shortwave flux is 321 W m^{-2}, compared with 314 W m^{-2} in GERB. It is -290 W m^{-2} for net longwave, with -276 W m^{-2} in GERB, giving 31 W m^{-2} for net radiation, compared with 38 W m^{-2} in GERB, i.e. there is more shortwave heating in the model, with more longwave cooling, giving less net TOA heating. These RT model shortwave/longwave/net (SW/LW/N) biases of 7/-14/-7 W m^{-2} although larger than many of the sensitivity ranges for the input data uncertainties (Table 1) are within the estimated error of the GERB measurements (~15 W m^{-2}, Ansell et al., 2014). It is difficult to identify the most important sources of this bias although errors in the reanalysis skin temperature and ERA-I cloud representation included in the wDwC experiment are likely candidates. The DRE of cloud provides a useful comparison and could be considered to be an estimate of the upper limit of cloud-related biases. Cloud DRE (Table 2~~4~~5) is estimated from the difference in fluxes at the TOA between wDnC and wDwC to be -4/7/3 W m^{-2} and from EBFA-CERES to be -15/16/1 W m^{-2}. These results of cloud DRE indicate that the optimum configuration flux biases are within the uncertainties of both observations and cloud effects. Despite the fact we used a set of input data resulting in simulation of radiative flux closest to observation and thus reduced the resulting error, it is necessary to note there still exists uncertainties ~~,~~raising error in the flux calculations. For example uncertainty in dust size distribution ~~sensitivity experiments made using the two different size distribution of dust resulted~~could result in ~~in~~ 25 W m^{-2} bias ~~in TO A shortwave flux~~ and small fractional difference in surface albedo could bring an error of 16 W m^{-2} in TOA shortwave flux (Table S1).

At the surface ~~-~~there is a relatively wider disparity between simulated and observed flux (Table 3~~4~~). The net shortwave simulated flux, 187 W m^{-2}, is 7 W m^{-2} more than measured surface shortwave flux. Net longwave flux is -103 W m^{-2} compared with that of measurement -78 W m^{-2}, the net effect being more cooling at the surface in the model than measurement by 25 W m^{-2}. We can again give comparison of cloud related biases between our result and CERES-EBFA product. Cloud SW/LW/N DRE at surface is estimated as -5/3/-2 W m^{-2} from the wDwC-wDnC experiments and -19/11/-8 W m^{-2} from EBFA-CERES, such that the shortwave bias at least could be explained by cloud but not all the longwave or net radiation bias. The remaining error could be attributable to measurement related errors and uncertainties to other variables such as surface emissivity, skin temperature, and surface albedo. For instance in our sensitivity experiments we found bias in net surface longwave flux by 6 W m^{-2} (Table S1) due to difference of mean skin temperature 1 K between Era-I and MERRA data. Further we found uncertainty in emissivity by 0.05 resulting in 5 W m^{-2} changes in surface

longwave flux. Note also the difference in time averaging periods between the CERES-EBFA data covering whole of June 2011 and the RT experiments wDwC-wDnC covering for 8th-30th June could possibly contribute to part of the differences in the above figures.

RT model bias in the longwave is larger than that in the shortwave at both TOA and surface. The mean diurnal cycle of flux bias (~~Figure~~Fig. 8) shows that modelled outgoing longwave flux is overestimated at night time. Different factors could be attributed to this difference. Surface skin temperature used in this work is interpolated to 1 hr (~~Figure~~Fig. ~~4~~6), which could lead to errors in the longwave flux. Satellite observations (see Marsham et al., (2013b)) show over both shallow cumulus cloud at the top of the PBL during late afternoon and occasional moist convection preferentially at night, which may be missed in models given the poor representation of moist convection. This could also contribute to the difference between observed and calculated longwave flux associated with under-representation of cloud in the model.

The RT simulation wDwC captures well the day-to-day variability in radiative fluxes at TOA and surface (~~Figure~~Fig. 9) including the effect of the major synoptic and meso-scale dust/water vapour events e.g. the haboob event of 21st June. However, in the longwave there are significant RT model errors during the night time of 17th and 18th June, which are cases of high dust load following haboob events. Analysis of satellite imagery shows this anomalous high GERB longwave flux to be coincident with convective cloud development, presumably resulting from the moistening of the Saharan atmosphere, which the RT model, dependent on reanalysis cloud field, cannot capture. This coincidence of dust and cloud is particularly challenging for both GERB cloud screening (which fails in this instance hence our use of all sky observations) and for the RT simulations themselves. A stronger anomalous flux from the diurnal mean in GERB measurements compared with wDwC result and CERES measurements for the wDwC simulation and observation can be clearly seen in Fig. S2a and Fig. S2b.

We can evaluate our model wDnC experiment results against clear-sky CERES footprint data in which RMSE are 17 W m^{-2} and 12 W m^{-2} for TOA shortwave and longwave fluxes, respectively. The equivalent figures for the model versus GERB (cloud screened using the CERES footprint cloud mask product) at the same times are 22 W m^{-2} and 12 W m^{-2}. These are comparable to and consistent with (i) the individual instrumental errors of CERES/GERB (ii) the inter-sensor uncertainties (CERES vs GERB RMSE = 22 W m^{-2} and 6 W m^{-2} for shortwave and longwave) (iii) previous similar studies (e.g. Osipov et al., 2015).

In summary, RT simulated flux errors of the 'optimum' configuration are comparable to observational uncertainties and those errors introduced by uncertainties in input fields. On this basis we suggest the RT configuration is acceptable for further analysis on the direct radiative effect of dust and water vapour.

4.2. The radiative flux and heating effects of dust and water vapour

First, we consider the TOA and surface mean radiative budgets. In the absence of dust and cloud the Saharan atmosphere during June~~summer~~ 2011 at BBM shows a positive radiation budget at the surface of 99 W m^{-2} in which shortwave heating of 237 W m^{-2} is offset by longwave cooling of -138 W m^{-2} (Table ~~3~~4). At TOA the shortwave flux of 328 W m^{-2} is not quite offset by longwave losses of 313 W m^{-2} (Table ~~2~~3) leading to a net positive radiation balance of 15 W m^{-2} making the SHL a weak net radiation sink. This strong (weak) radiation surplus at surface (TOA) leads to the atmosphere having a net cooling of 83 W m^{-2} (i.e. radiative divergence),

Formatted: Superscript
Formatted: Superscript

presumably maintained by the transfer of sensible heat from surface into the atmosphere through turbulent heat transfer (Alamirew et al., submitted).

Both dust and water vapour are known to play an important role in controlling the radiative budget and heating rate of surface and the atmosphere over Sahara. Variability in these two active radiative components is strongly correlated due to the physical processes that govern transport of water vapour and dust emission into the SHL region (Marsham et al., 2013b; M16) such that it is challenging to quantify their separate radiative effects from observations alone. Our RT simulations below address this research gap.

4.2.1 Dust

Here we determine the DRE of dust using two set of experiments described in Table 12. First we compare the simulations of radiative fluxes and heating during June 2011 between the wDnC and nDnC experiments (~~Figure~~Fig.~~s~~ 10, Fig. 11, Fig. – 12, and Fig. 13 and Table 24~~s 3 and 4~~). Secondly, we derive~~d~~ the sensitivity of radiative fluxes and heating rates to a wide range of dust AOD using the sensitivity experiments (Fig~~ure~~ 112). We then compare our estimates of dust DRE to those from previous studies.

The mean SW/LW/N DRE of dust at TOA for June 2011 estimated from wDnC minus nDnC is -3/16/13 W m^{-2} confirming the net warming effect of dust over the Sahara. This warming comes primarily in the longwave with a peak at ~24 W m^{-2} close to midday (~~Figure~~Fig. 10a). The net shortwave DRE is small, consistent with other estimates (Huang et al., 2014; Yang et al., 2009). However, with a pronounced diurnal structure driven by a semi-diurnal cycle in the shortwave with a cooling effect of up to -29 W m^{-2} after dawn until 10:00 and after ~16:00 until sunset, and a warming effect of up to ~22 W m^{-2} around midday (~~Figure~~Fig. 10a). The diurnal cycle of dust DRE is not strongly dependent on the amount of dust loading in the atmosphere but controlled by solar zenith angle and surface albedo (Ansell et al., 2014; Banks et al., 2014). The phase function also exerts a control on the diurnal cycle of the DRE as its value increases the backscatter fraction of SW radiation at large solar zenith angles. For comparison, the equivalent TOA SW/LW/N DRE of dust for MERRA reanalysis are 10/7/17 W m^{-2} suggesting that although MERRA has a good estimate of net DRE but the apparent shortwave warming effect is not in agreement with observations and the longwave warming is underestimated.

At the surface the SW/LW/N DRE of dust is estimated to be -45/32/-13 W m^{-2} for SW/LW/N (Table 345). The net cooling is driven by the shortwave which peaks at ~-108 W m^{-2} around noon (~~Figure~~Fig. 10b) partly compensated by a longwave heating effect of 32 W m^{-2}. The MERRA reanalysis DRE at surface is -30/20/-12 W m^{-2} again showing a good estimate of net effects but underestimating the shortwave and longwave components. The time series of shortwave DRE of dust (see supplementary material Fig. S3a~~Figure 11a~~) at TOA further confirms the diurnal cycle discussed above: a midday warming and early morning and late afternoon cooling. The impact of big dust events (e.g. June 17th and 21st) can be clearly seen on the time series of longwave DRE of dust (~~Figure~~Fig. S~~1~~31~~b~~).

The results of sensitivity experiments 'senDnC' are shown in ~~Figure~~Fig. 12~~2~~1 and the DRE per unit AOD and per unit standard deviation in AOD is presented in Table 45~~6~~, assuming a linear relationship between flux and AOD with regressions provided at 95% confidence interval. We find the net TOA shortwave flux to be only weakly sensitive to dust AOD (~~Figure~~Fig. 112 (d) at -1.8±0.12 W m^{-2} per AOD. This is due to the

competing dust effect of increasing surface albedo which decreases net TOA shortwave and absorption by dust which increases TOA net shortwave by reducing the upwelling shortwave radiation. Our estimates of shortwave dust DRE is less than half the sensitivity reported at BBM by M16, but consistent with the Sahara-wide estimates from satellite of Yang et al., (2009) and those of Ansell et al., (2014).

Dust in the atmosphere acts to reduce the outgoing longwave flux by 10.0±0.4 W m^{-2} per unit increase in AOD (~~Figure~~Fig. 1~~2~~a), warming the surface, consistent with the observations at BBM of M16 (11 W m^{-2} per AOD increase) and within the Sahara-wide range of Yang et al., (2009).

At the surface dust has opposing effect in shortwave and longwave, with shortwave having stronger cooling effect: for every unit increase in AOD there is shortwave reduction (~~Figure~~Fig. 1~~2~~e, Table 6) of 3~~3.8±1.34~~W m^{-2} compared to increase in longwave (~~Figure~~Fig. 1~~2~~1b) with 19.7±1.4~~20~~ W m^{-2} the net effect (~~Figure~~Fig. 1~~2~~h) being cooling of -14.1±0.1 W m^{-2} per AOD increase.

Dust drives radiative convergence in the atmosphere i.e. the difference in TOA minus surface flux, which acts to warm the atmosphere. This occurs through greater shortwave absorption, at a rate of 32.1±1.4 W m^{-2} per AOD (~~Figure~~Fig. 1~~2~~f) offset partially by longwave cooling the atmosphere at -9.7±1.0~~10~~ W m^{-2} per unit AOD increase, leading to a net warming effect of 22.4±0.4 W m^{-2} per unit change in AOD. Overall, the RT estimates of TOA and Surface DRE in the shortwave and longwave and the atmospheric radiative convergence are within a few W m^{-2} of those of M16 derived from observations.

We convert the radiative fluxes to actual heating rates (~~Figure~~Fig. 1~~2~~3a). In the absence of dust (nDnC experiment) the PBL is heated in the shortwave mainly from absorption by O_2 and water vapour peaking up to ~1.3 K day^{-1} at 450 hPa (the water vapour effect is shown in ~~Figure~~Fig. 1~~4~~5). Strong longwave cooling throughout the troposphere (up to ~-3 K day^{-1} at ~450 hPa) due to emission from water vapour and other greenhouse gases exceeds this shortwave heating, leading to tropospheric radiative cooling of ~-0.6 K day^{-1} throughout the PBL. This is consistent with the radiative heating estimate of Alamirew et al. (submitted) derived as a residual of the heat budget. In the lowest near surface layer (below 925 hPa) there is less longwave cooling due to strong radiative flux from the hot desert surfaces in the SHL. Dust acts to modify the vertical structure of this radiative heating/cooling considerably. Absorption of shortwave radiation leads to a strong warming effect in the shortwave (especially in the dusty PBL up to ~0.75 K day^{-1} below ~700 hPa, where dust loadings are the highest), offset only partially by enhanced longwave cooling (up to ~-0.25 K day^{-1}) resulting in a net warming of the atmosphere by up to ~0.5 K day^{-1} at ~700hPa, such that the dusty troposphere above ~600hPa has near zero cooling. For comparison we consider the MERRA reanalysis product mean heating rate (~~Figure~~Fig. 1~~2~~3b), which includes both cloud and climatological dust, is in close agreement with those of the wDwC experiment. However, MERRA does not capture the day-to-day variability in shortwave heating from dust and will not therefore be able to simulate the responses of the SHL atmosphere to variability at these timescales. Further weather/climate model simulations are required to determine the effect this has on the regional circulation and the behaviour of the SHL.

Day-to-day variability in the dominant shortwave net heating rate (~~Figure~~Fig. 1~~3~~4) is pronounced and shows the impact of the synoptic/meso-scale dust events on the SHL atmosphere. During large dust events (e.g. June 17th and 21st~~,~~) there is strong shortwave heating up to 6 K day^{-1} around midday hours. This will be coincident with reduced surface net radiation and sensible heat flux. Together these processes will act to reduce

Formatted: Indent: First line: 1.27 cm

the vertical temperature gradient, stabilise the atmosphere, reduce dry convection and reduce the depth of the PBL.

4.2.2 ~~water~~Water vapour

To estimate the heating rate profiles due to water vapour, we selected from the simulation nDnC the three driest days (June 11, 12, and 16) with mean column integrated water vapour of 20.2 Kg m^{-2} and three most humid days (June 18, 25, and 30) with mean column integrated water vapour of 34.7 Kg m^{-2}. The mean heating rate profiles for the two contrasting atmospheric conditions is shown in ~~Figure~~Fig. 1~~4~~5. High humidity drives an increase in the shortwave heating rate up to 0.5 K day^{-1} peaking near the surface. This atmospheric warming is counteracted by a slightly bigger cooling in the longwave. Thus there is a net cooling up to -0.25 K day^{-1} in atmospheric and strong heating up to 2.5 K day^{-1} near the surface as a result of increase in moisture. The atmospheric cooling in the longwave causes surface warming, which is suggested to be linked with the intensification of the Saharan heat low region (Evan et al., 2015b). The reversed heating rate profiles in the layer between 500 hPa and 400 hPa is because of the mean moisture profile in this layer is larger during the dry days and the vice versa (F~~f~~igure 2).

Results from the water vapour sensitivity experiments 'senWVwDnC' are presented in ~~Figure~~Fig. 1~~5~~6 and the linear dependence on fluxes per unit water vapour in Table ~~4~~5~~5~~6. We again present the regression values to 95% confidence level. The outgoing longwave radiation (~~Figure~~Fig. 1~~5~~6a) decreases with increasing of water vapour at a rate 1.1±0.7 W kg^{-1} which is associated with the greenhouse effect of water vapour. This is about a third of that derived by M16 (3 W kg^{-1}). Their result includes the effect of water vapour and associated dust and cloud while our result considers sensitivity of radiative flux to changes in water vapour only. The sensitivity of TOA shortwave flux due to water vapour (~~Figure~~Fig. 1~~5~~6d) is 0.3±0.3 W Kg^{-1} which warms the atmosphere and to the contrary cools the surface due to the reduction of the shortwave reaching the earth. M16 showed that a reduction in the TOA shortwave radiation with increasing of water vapour, of -0.98 W Kg^{-1} which is contrary to what we find in our results. But this could be related with ~~to~~ the impact of cloud on ~~the~~ shortwave radiation which will reduce ~~the~~ TOA net shortwave radiation. The net flux at TOA increases by to 1.4 W m^{-2} for a unit change in CIWV resulting in a net warming of the TOA.

The net flux reaching the surface (~~Figure~~Fig. 1~~5~~6h) is increased at a rate 1.1±0.4 W Kg^{-1} which is the counteracting effect of a dominant increase in longwave radiation re-emitted downwards from the atmosphere (1.5±0.8 W Kg^{-1}) and a smaller reduction in downwelling solar radiation (-0.4±0.4 W Kg^{-1}). The warming effect of water vapour at both the surface and the TOA means that net atmospheric convergence changes relatively little with water vapour (~~Figure~~Fig. 1~~5~~6i) at 0.3±0.6~~1~~ W Kg^{-1} which is a result of -0.~~5~~6±0.1 W Kg^{-1} in the longwave (~~Figure~~Fig. 1~~5~~6c) and 0.8±0.7~~7~~ W Kg^{-1} in the shortwave (~~Figure~~Fig. 1~~5~~6f). In comparison to the observational analysis of M16 we see some important differences, notably we see a greater surface net warming effect of water vapour and as a result negligible, not positive atmospheric radiation convergence. Nevertheless our estimate of the sensitivity of surface longwave radiation to changes in CIWV of 1.1 W Kg^{-1} is at the lower end of the range (1.0 - 3.6 W Kg^{-1}) estimated by Evan et al., (2015b), from observations and RT simulations, suggesting the role of water vapour in driving longer term interannual to decadal heating of the SHL may not be as pronounced as previously suggested.

4.2.3. The relative effects of dust versus water vapour

From the sensitivity experiments, we can quantify the DRE of dust and water vapour at TOA and surface per unit change in AOD dust and kg water vapour respectively (Table 456). By scaling this to observed standard deviation in each variable observed during the Fennec observation period we provide estimates of the relative importance of dust and water vapour to the day-to-day variability in the radiation budget over the SHL.

The resulting normalised dust SW/LW/net DRE per AOD at TOA and surface is -1/8/7 W m^{-2} and -27/16/-11 W m^{-2} respectively, where these figures provide a useful way of presenting the variability of dust and water vapour on their radiative effects. The equivalent values for water vapour are 2/6/8 W m^{-2} and -2/8/6 W m^{-2}. As such, the radiative effects of dust and water vapour at TOA are of similar magnitude with net warming of ~7 W m^{-2} per unit variability. Dust and water vapour exert similar control on the total heating of the Earth-atmosphere. This contrasts with M16 who report water effects (from vapour and cloud) as ~3 times more powerful than dust. This is an important finding of this paper signifying the role of particularly dust in controlling the variability of radiative flux and therefore heat budget of the region.

At the surface radiative flux is controlled much more strongly by dust than water vapour and with opposite sign: net cooling of -11 W m^{-2} and warming of 6 W m^{-2} per unit variability respectively. M16 find near zero warming from water (vapour and cloud). In our study the net effect of TOA versus surface is strong atmospheric warming of 18 W m^{-2} per unit variability from dust and negligible warming (1 W m^{-2} per unit variability) from water vapour. In contrast, M16 find almost equal warming from dust and water vapour (of 11-12 W m^{-2} per unit variability). Although this radtiative transfer based analysis of the role of water vapour does not include ~~the~~ cloud that is implicitly included in M2016, we suggest that the co-variability of dust and water vapour hinders calculation of their independent effects in the observational analysis of M16.

In summary we find that dust and water vapour exert a similarly large control on TOA net radiation and therefore total column heating and by implication to the first order similar control on surface pressure in the SHL. However, the vertical structure of radiative heating from dust is far more complex than that for water vapour. The schematic, ~~Figure~~Fig. 16~~7~~ and Fig. 17 illustrate~~s~~ the sensitivity of dust and water vapour respectively at different pressure levels. The grey shading in fig. 16 (fig. 17) represents amount of dust (water vapour) which ~~at each will~~ give~~s the~~ AOD (CIWV) values shown on the horizontal axis when vertically summed. Dust imposes a strong net cooling at the surface from the SW which declines to zero at ~700hPa, where SW cooling and LW warming balance, with net warming above this (Table 456). In contrast water vapour imposes a LW heating effect that varies relatively little from surface to TOA. As such dust is likely to have stronger impact on the structure and processes of the SHL atmosphere than does water vapour.

5. Summary and Conclusions

The summertime Saharan Heat Low feature is of considerable importance to the wider regional climate over West Africa but remains poorly understood. To the first order the SHL is created by strong sensible heat flux from the surface radiative surplus which heats the deep Saharan boundary layer, which is in near balance with advective cooling from the low level convergence circulation. However, radiative heating is modulated by

water vapour and dust whose variations, at least at short timescales, are correlated. Here, we aim to quantify the independent radiative effects of dust and water vapour, and the vertical profile of atmospheric heating rates using an RT model. The model is configured for the location at BBM, close to the heart of the SHL using inputs from Fennec field campaign for June 2011. First, sensitivity to uncertainty in RT model inputs fields is assessed. We find that dust size distribution is the most important source of uncertainty in this case, through its impact on single scattering albedo. The RT model when suitably configured has radiative flux biases at TOA that are within observational uncertainties and input uncertainties. The subsequent RT experiments show:

1. ~~1.~~ On average the SHL has a large positive radiative surplus at surface of 83 W m^{-2}, a small surplus at TOA of 31 W m^{-2} with a net atmospheric radiative divergence of 52 W m^{-2} presumably approximately balanced by the transfer of sensible heat.

2. ~~2.~~ The effect of dust is pronounced:
   I. D~~D~~uring June 2011 dust had a positive DRE at TOA of 8 W m^{-2} per unit AOD (7 W m^{-2} per unit AOD variability) almost entirely in the longwave, as the effects of shortwave absorption with respect to surface albedo largely balance, acting to warm earth-atmosphere system as a whole, with magnitude consistent with previous studies (Banks et al., 2014; M16; Yang et al., 2009).
   II. Dust has a strong negative DRE at the surface of -14 W m^{-2} per unit AOD (-11 W m^{-2} per unit AOD variability) largely due to reduced shortwave flux from atmospheric absorption.
   III. The net effect of this negative surface DRE and positive TOA DRE is considerable atmospheric radiative convergence of 22 W m^{-2} per unit AOD (18 per unit AOD variability) largely from shortwave absorption. This directly heats the PBL below ~500hPa by ~0.6 K day^{-1}.
   IV. Dust loading is variable and the heating effect of episodic synoptic and meso-scale dust events can be up to 6 K day^{-1}.

3. ~~3.~~ The effect of water vapour is weaker than dust at the surface and includes:
   I. a positive radiative effect at TOA of 1.4 W m^{-2} per unit column integrated water vapour (8 W m^{-2} per unit water vapour variability) almost entirely a longwave greenhouse effect.
   II. a weak positive radiative effect at the surface of 1.2 W m^{-2} per unit column integrated water vapour (6 W m^{-2} per unit water vapour variability) almost entirely from longwave radiation re-emitted downwards.
   III. positive radiative effects at surface and TOA and thus a negligible impact on atmospheric radiative convergence.

A key finding here is that in contrast to previous analysis dust and water vapour are roughly equally important at the TOA, in controlling day-to-day variability in heating the earth-atmosphere system as a whole, (in contrast to M16 who identify water and associated cloud as the key driver), but that dust variability dominates variations in surface and atmospheric radiative heating. The biggest single net radiative effect in this study is the atmospheric radiative convergence from dust. The impact of dust may therefore be greater than previously believed. Recent studies have proposed a water vapour positive-feedback mechanism driving decadal variations in SHL intensity, implicated in the recent recovery of Sahelian rainfall (Evan et al., 2015b). Our

Formatted: Numbered + Level: 1 + Numbering Style: 1, 2, 3, … + Start at: 1 + Alignment: Left + Aligned at: 0.63 cm + Indent at: 1.27 cm

Formatted: Numbered + Level: 1 + Numbering Style: 1, 2, 3, … + Start at: 1 + Alignment: Left + Aligned at: 0.63 cm + Indent at: 1.27 cm

results are consistent with this but strongly suggest that variability in dust loading should be considered in explaining variability and change in the SHL, reinforcing the need for high quality long term aerosol observations. Additionally dust size distributions, shape and chemical composition are spatially and temporally variable, and the vertical profile of dust will vary with meteorological conditions – thus introducing more variability and uncertainty than has been explored in this study. These variations potentially increase the controls of dust on the radiation budget even further than quantified here.

Therefore, water vapour events in themselves act to heat at the TOA and at the surface and presumably intensify the SHL. In contrast, dust events cool the surface but warm the lower troposphere as a whole, such that the net effect at the top of the Saharan residual layer (about 5km) is a warming which will intensify the SHL. Various climate model experiments also demonstrate this effect (Mulcahy et al., 2014). We can then consider the effects of variability in SHL associated with monsoon surges and haboobs in which dust and water vapour increases are often coincident. Through radiative processes such events act to (i) warm the whole troposphere, almost equally through dust and water vapour longwave effect (ii) strongly cool the surface from dust shortwave effect, and more weakly warm the surface through water vapour longwave effects. Although these counteracting effects mean the net surface radiative flux reduction is actually quite small, the diurnal effects are pronounced with the dust shortwave apparent in daytime and the water vapour effect dominant at night, which will act to reduce the sensible heat flux into the atmosphere limiting the vertical development of the SHL PBL (iii) Substantial radiative heating from dust occurs in the PBL up to 6 K day^{-1} through dust shortwave absorption. This will act to stabilise the PBL with implications for dry and moist convection, although Trzeciak et al. (2017) suggest that moistening may often counter this. Such events typically involve an additional advective cooling which can be substantial up to 2-5 K day^{-1} for monsoon surges (Couvreux et al., 2010) but is restricted to the lowest layers (~1 km from surface).

Couvreux et al. (2010) suggested a negative feedback process within the SHL-monsoon systems that may govern preferred 3-5 day timescale of variability in the SHL and monsoon pulses. Strong net radiative heating at the surface intensifies the SHL, enhancing monsoon surges which then, through low level advective cooling, act to weaken the SHL, before solar heating restores the SHL. Our results add potentially important detail regarding the radiative role of dust and water vapour that may modify this conceptual understanding. First, the net effect on surface radiation of dust and water vapour together is to further cool the surface and weaken the SHL, in addition to the advective cooling. Second, this weakening of the SHL is offset because the magnitude of dust radiative heating in the lowest layers is comparable to that of advective cooling so that net effect may be small or even positive, but with the dust radiative heating extending throughout the entire PBL above, rather than just the lowest 1km or so. Third, the timescale of re-establishment of the SHL through surface heating and sensible heat flux may be influenced by the rate of dust deposition and export, which, depending on the synoptic context may be 1-2 days, though sometimes dust remains suspended in the SHL for days -weeks. The net effect of these, often competing, processes on the SHL will depend on the precise nature of water vapour, dust and temperature advection during such monsoon surge events. As such, SHL variability will represent a complex interplay of factors rather than a feedback through a single mechanism. There is a clear need for much better spatially extensive and detailed observations of all these variables. Given the limited temporal and spatial coverage of our study such inferences are necessarily speculative and a full and rigorous analysis of SHL variability in response to advective and radiative drivers would require further analysis.

Formatted: English (U.K.)

We can therefore envisage an inherent tendency for pulsing in the SHL in which an intensifying SHL will lead towards monsoon surges, which act through near surface/low level radiative and advective cooling to weaken the SHL and through dust-radiative heating to stabilise the PBL, until dust deposition and export allow re-warming of the surface to re-invigorate the SHL.

Given the radiative effects described above the dynamical effects of dust variability on the low level convergence and mid-level divergence circulations will be greater than those of water vapour and require further model experiments to resolve. Whilst reanalysis models represent well the average radiative and heating effect of dust and water vapour they do not capture dust and water vapour variability well and the subsequent dynamical effects on the larger scale circulation.

The unique observations of the Fennec aircraft campaign suggested that fresh dust is much coarser than previously believed (Ryder et al., 2013b), with corresponding higher absorption, and this has significant impacts on the radiation budget (Kok et al., 2017). Our RT model simulations results suggest that such a dominant coarse mode is not consistent with TOA radiative flux observations at BBM. However, if dust is coarser than we assume here then the radiative effects of dust would be even stronger. Further observations on dust size distribution and optical properties are a priority requirement. In addition, further work should consider in much greater detail the radaitive effects of cloud based on detailed observations rather than the rather coarse estimates from reanalysis used here.

Our results showing the complex interplay of dust and water vapour on surface and PBL radiative heating stress the need for improved modelling of these processes over the SHL region to improve predictions including those for the WAM across timescales (e.g. Evan et al., 2015). Most models currently struggle in regard to short term variability in water vapour (Birch et al., 2014; Garcia-Carreras et al., 2013; Marsham et al., 2013a; Roberts et al., 2015), clouds (Roehrig et al., 2013; Stein et al., 2015) and dust (Evan et al., 2014), with many dust errors coming from moist convection (Heinold et al., 2013; Marsham et al., 2011). Forecast models typically have mean biases of up to 2 kg m^{-2} in column integrated water vapour (equivalent to change in 2.6 W m^{-2} TOA net flux) and lack variability in dust, and so are expected to poorly represent these couplings. A focus on improved representation of advection of water vapour, clouds and convection in models should be a priority.

This paper has provided insight into the separate and combined roles of water vapour and dust in controlling the variability of the summertime radiative flux and heating rate over the SHL region. We recognise that generalising across all the SHL region for all summer months is problematic from one particular point and the short period of our study. Furthermore there still remains uncertainty in input dataset which includes surface characteristics and cloud. It is therefore necessary to have a more comprehensive dataset to reduce these uncertainties and thus improve quantitative results. Further research is thus necessary to confirm the results of our limited study spanning longer period of time and bigger domain.

Acknowledgements

This research was funded through the Peter Carpenter African Climate scholarship, further supported by UK NERC consortium grant NE/G017166/1. We would like to acknowledge data provided from NERC-funded FENNEC project. Helen Brindley has given us constructive suggestions that were important to complete this research. We thank Jamie Banks for providing processed GERB TOA radiation data and Adriana Rocha-Lima for providing Nephelometer measured dust optical properties data. We would like to thank Azzendine Saci, Abdelkader Ouladichir, Bouzianne Ouchene, Mohammed Salah-Ferroudj, Benyakoub Abderrahmane, Mohammmed Limam, and Diali Sidali (ONM) and Richard Washington (University of Oxford) for their contributions to setting up running the Fennec supersite, and indeed all at ONM Algeria for their patience and hospitality during Fennec. We would like to thank the AERONET PHOTONS team for their assistance with the Cimel Sun photometer. The authors also would like to thank Eleanor Highwood for facilitating access to computational cluster at Metrology Department in University of Reading.

References

Alamirew, N. K., Todd M., Washington R., Wang, Y., 2017. The Heat and Moisture budget over the Saharan Heat Low (submitted manuscript)

Anderson, G. P., Clough, S. A., Kneizys, F. X., Chetwyn, J. H., and Shettle, E. P 1986. Atmospheric constituent profiles (0 –120 km). Technical Report AFGL-TR-86-0110, AFGL (OPI), Hanscom AFB, MA. 01736

Ansell, C., Brindley, H. E., Pradhan, Y. & Saunders, R. 2014. Mineral dust aerosol net direct radiative effect during GERBILS field campaign period derived from SEVIRI and GERB. *Journal of Geophysical Research-Atmospheres,* 119**,** 4070-4086.

Banks, J. R. & Brindley, H. E. 2013. Evaluation of MSG-SEVIRI mineral dust retrieval products over North Africa and the Middle East. *Remote Sensing of Environment,* 128**,** 58-73.

Banks, J. R., Brindley, H. E., Hobby, M. & Marsham, J. H. 2014. The daytime cycle in dust aerosol direct radiative effects observed in the central Sahara during the Fennec campaign in June 2011. *Journal of Geophysical Research-Atmospheres,* 119**,** 13861-13876.

Birch, C. E., Marsham, J. H., Parker, D. J. & Taylor, C. M. 2014. The scale dependence and structure of convergence fields preceding the initiation of deep convection. *Geophysical Research Letters,* 41**,** 4769-4776.

Chauvin, F., Roehrig, R. & Lafore, J. P. 2010. Intraseasonal Variability of the Saharan Heat Low and Its Link with Midlatitudes. *Journal of Climate,* 23**,** 2544-2561.

Couvreux, F., Guichard, F., Bock, O., Campistron, B., Lafore, J. P. & Redelsperger, J. L. 2010. Synoptic variability of the monsoon flux over West Africa prior to the onset. *Quarterly Journal of the Royal Meteorological Society,* 136**,** 159-173.

Dee, D. P., Uppala, S. M., Simmons, A. J., Berrisford, P., Poli, P., Kobayashi, S., Andrae, U., Balmaseda, M. A., Balsamo, G., Bauer, P., Bechtold, P., Beljaars, A. C. M., van de Berg, L., Bidlot, J., Bormann, N., Delsol, C., Dragani, R., Fuentes, M., Geer, A. J., Haimberger, L., Healy, S. B., Hersbach, H., Holm, E. V., Isaksen, L., Kallberg, P., Kohler, M., Matricardi, M., McNally, A. P., Monge-Sanz, B. M., Morcrette, J. J., Park, B. K., Peubey, C., de Rosnay, P., Tavolato, C., Thepaut, J. N. & Vitart, F. 2011. The ERA-Interim reanalysis: configuration and performance of the data assimilation system. *Quarterly Journal of the Royal Meteorological Society,* 137**,** 553-597.

Dong, B. W. & Sutton, R. 2015. Dominant role of greenhouse-gas forcing in the recovery of Sahel rainfall. *Nature Climate Change,* 5**,** 757-U173.

Dubovik, O., Holben, B., Eck, T. F., Smirnov, A., Kaufman, Y. J., King, M. D., Tanre, D. & Slutsker, I. 2002. Variability of absorption and optical properties of key aerosol types observed in worldwide locations. *Journal of the Atmospheric Sciences,* 59**,** 590-608.

Edwards, J. M. & Slingo, A. 1996. Studies with a flexible new radiation code .1. Choosing a configuration for a large-scale model. *Quarterly Journal of the Royal Meteorological Society,* 122**,** 689-719.

Evan, A. T., Flamant, C., Fiedler, S. & Doherty, O. 2014. An analysis of aeolian dust in climate models. *Geophysical Research Letters,* 41**,** 5996-6001.

Evan, A. T., Fiedler, S., Zhao, C., Menut, L., Schepanski, K., Flamant, C. & Doherty, O. 2015a. Derivation of an observation-based map of North African dust emission. *Aeolian Research,* 16**,** 153-162.

Evan, A. T., Flamant, C., Fiedler, S. & Doherty, O. 2014. An analysis of aeolian dust in climate models. *Geophysical Research Letters,* 41**,** 5996-6001.

Evan, A. T., Flamant, C., Lavaysse, C., Kocha, C. & Saci, A. 2015b. Water Vapor-Forced Greenhouse Warming over the Sahara Desert and the Recent Recovery from the Sahelian Drought. *Journal of Climate,* 28**,** 108-123.

Garcia-Carreras, L., Marsham, J. H., Parker, D. J., Bain, C. L., Milton, S., Saci, A., Salah-Ferroudj, M., Ouchene, B. & Washington, R. 2013. The impact of convective cold pool outflows on model biases in the Sahara. *Geophysical Research Letters,* 40**,** 1647-1652.

Greed, G., Haywood, J. M., Milton, S., Keil, A., Christopher, S., Gupta, P. & Highwood, E. J. 2008. Aerosol optical depths over North Africa: 2. Modeling and model validation. *Journal of Geophysical Research-Atmospheres,* 113.

Harries, J. E., Russell, J. E., Hanafin, J. A., Brindley, H., Futyan, J., Rufus, J., Kellock, S., Matthews, G., Wrigley, R., Last, A., Mueller, J., Mossavati, R., Ashmall, J., Sawyer, E., Parker, D., Caldwell, M., Allan, P. M., Smith, A., Bates, M. J., Coan, B., Stewart, B. C., Lepine, D. R., Cornwall, L. A., Corney, D. R., Ricketts, M. J., Drummond, D., Smart, D., Cutler, R., Dewitte, S., Clerbaux, N., Gonzalez, L., Ipe, A., Bertrand, C., Joukoff, A., Crommelynck, D., Nelms, N., Llewellyn-Jones, D. T., Butcher, G., Smith, G. L., Szewczyk, Z. P., Mlynczak, P. E., Slingo, A., Allan, R. P. & Ringer, M. A. 2005. The

geostationary Earth Radiation Budget Project. *Bulletin of the American Meteorological Society,* 86**,** 945-+.

Heinold, B., Knippertz, P., Marsham, J. H., Fiedler, S., Dixon, N. S., Schepanski, K., Laurent, B. & Tegen, I. 2013. The role of deep convection and nocturnal low-level jets for dust emission in summertime West Africa: Estimates from convection-permitting simulations. *Journal of Geophysical Research-Atmospheres,* 118**,** 4385-4400.

Holben, B. N., Eck, T. F., Slutsker, I., Tanre, D., Buis, J. P., Setzer, A., Vermote, E., Reagan, J. A., Kaufman, Y. J., Nakajima, T., Lavenu, F., Jankowiak, I. & Smirnov, A. 1998. AERONET - A federated instrument network and data archive for aerosol characterization. *Remote Sensing of Environment,* 66**,** 1-16.

Huang, J. P., Wang, T. H., Wang, W. C., Li, Z. Q. & Yan, H. R. 2014. Climate effects of dust aerosols over East Asian arid and semiarid regions. *Journal of Geophysical Research-Atmospheres,* 119**,** 11398-11416.

Knippertz, P. & Todd, M. C. 2012. Mineral Dust Aerosols over the Sahara: Meteorological Controls on Emission and Transport and Implications for Modeling. *Reviews of Geophysics,* 50.

Lafore, J. P., Flamant, C., Giraud, V., Guichard, F., Knippertz, P., Mahfouf, J. F., Mascart, P. & Williams, E. R. 2010. Introduction to the AMMA Special Issue on 'Advances in understanding atmospheric processes over West Africa through the AMMA field campaign'. *Quarterly Journal of the Royal Meteorological Society,* 136**,** 2-7.

Lavaysse, C., Flamant, C., Evan, A., Janicot, S., & Gaetani, M. (2016). Recent climatological trend of the Saharan heat low and its impact on the West African climate. *Climate Dynamics, 47*(11), 3479-3498. doi:10.1007/s00382-015-2847-z

Lavaysse, C., Flamant, C., Janicot, S., Parker, D. J., Lafore, J. P., Sultan, B. & Pelon, J. 2009. Seasonal evolution of the West African heat low: a climatological perspective. *Climate Dynamics,* 33**,** 313-330.

Liu, Z. Y., Vaughan, M., Winker, D., Kittaka, C., Getzewich, B., Kuehn, R., Omar, A., Powell, K., Trepte, C. & Hostetler, C. 2009. The CALIPSO Lidar Cloud and Aerosol Discrimination: Version 2 Algorithm and Initial Assessment of Performance. *Journal of Atmospheric and Oceanic Technology,* 26**,** 1198-1213.

Marsham, J. H., Knippertz, P., Dixon, N. S., Parker, D. J. & Lister, G. M. S. 2011. The importance of the representation of deep convection for modeled dust-generating winds over West Africa during summer. *Geophysical Research Letters,* 38.

Marsham, J. H., Parker, D. J., Grams, C. M., Taylor, C. M. & Haywood, J. M. 2008. Uplift of Saharan dust south of the intertropical discontinuity. *Journal of Geophysical Research-Atmospheres,* 113.

Marsham, J. H., Dixon, N. S., Garcia-Carreras, L., Lister, G. M. S., Parker, D. J., Knippertz, P. & Birch, C. E. 2013a. The role of moist convection in the West African monsoon system: Insights from continental-scale convection-permitting simulations. *Geophysical Research Letters,* 40**,** 1843-1849.

Marsham, J. H., Hobby, M., Allen, C. J. T., Banks, J. R., Bart, M., Brooks, B. J., Cavazos-Guerra, C., Engelstaedter, S., Gascoyne, M., Lima, A. R., Martins, J. V., McQuaid, J. B., O'Leary, A., Ouchene, B., Ouladichir, A., Parker, D. J., Saci, A., Salah-Ferroudj, M., Todd, M. C. & Washington, R. 2013b. Meteorology and dust in the central Sahara: Observations from Fennec supersite-1 during the June 2011 Intensive Observation Period. *Journal of Geophysical Research-Atmospheres,* 118**,** 4069-4089.

Formatted: French (France)

Formatted: English (U.S.)

Marsham, J. H., Knippertz, P., Dixon, N. S., Parker, D. J. & Lister, G. M. S. 2011. The importance of the representation of deep convection for modeled dust-generating winds over West Africa during summer. *Geophysical Research Letters,* 38.

Marsham, J. H., Parker, D. J., Grams, C. M., Taylor, C. M. & Haywood, J. M. 2008. Uplift of Saharan dust south of the intertropical discontinuity. *Journal of Geophysical Research-Atmospheres,* 113.

Marsham, J. H., Parker, D. J., Todd, M. C., Banks, J. R., Brindley, H. E., Garcia-Carreras, L., Roberts, A. J. & Ryder, C. L. 2016. The contrasting roles of water and dust in controlling daily variations in radiative heating of the summertime Saharan heat low. *Atmospheric Chemistry and Physics,* 16**,** 3563-3575.

Martin, E. R. & Thorncroft, C. 2014. Sahel rainfall in multimodel CMIP5 decadal hindcasts. *Geophysical Research Letters,* 41**,** 2169-2175.

Martin, E. R., Thorncroft, C. & Booth, B. B. B. 2014. The Multidecadal Atlantic SST-Sahel Rainfall Teleconnection in CMIP5 Simulations. *Journal of Climate,* 27**,** 784-806.

Messager, C., Parker, D. J., Reitebuch, O., Agusti-Panareda, A., Taylor, C. M. & Cuesta, J. 2010. Structure and dynamics of the Saharan atmospheric boundary layer during the West African monsoon onset: Observations and analyses from the research flights of 14 and 17 July 2006. *Quarterly Journal of the Royal Meteorological Society,* 136**,** 107-124.

Mulcahy, J. P., Walters, D. N., Bellouin, N. & Milton, S. F. 2014. Impacts of increasing the aerosol complexity in the Met Office global numerical weather prediction model. *Atmospheric Chemistry and Physics,* 14**,** 4749-4778.

Osborne, S. R., Baran, A. J., Johnson, B. T., Haywood, J. M., Hesse, E. & Newman, S. 2011. Short-wave and long-wave radiative properties of Saharan dust aerosol. *Quarterly Journal of the Royal Meteorological Society,* 137**,** 1149-1167.

Osipov, S., Stenchikov, G., Brindley, H. & Banks, J. 2015. Diurnal cycle of the dust instantaneous direct radiative forcing over the Arabian Peninsula. *Atmospheric Chemistry and Physics,* 15**,** 9537-9553.

Otto, S., Bierwirth, E., Weinzierl, B., Kandler, K., Esselborn, M., Tesche, M., Schladitz, A., Wendisch, M. & Trautmann, T. 2009. Solar radiative effects of a Saharan dust plume observed during SAMUM assuming spheroidal model particles. *Tellus Series B-Chemical and Physical Meteorology,* 61**,** 270-296.

Otto, S., de Reus, M., Trautmann, T., Thomas, A., Wendisch, M. & Borrmann, S. 2007. Atmospheric radiative effects of an in situ measured Saharan dust plume and the role of large particles. *Atmospheric Chemistry and Physics,* 7**,** 4887-4903.

Otto, S., Trautmann, T. & Wendisch, M. 2011. On realistic size equivalence and shape of spheroidal Saharan mineral dust particles applied in solar and thermal radiative transfer calculations. *Atmospheric Chemistry and Physics,* 11**,** 4469-4490.

Parker, D. J., Burton, R. R., Diongue-Niang, A., Ellis, R. J., Felton, M., Taylor, C. M., Thorncroft, C. D., Bessemoulin, P. & Tompkins, A. M. 2005. The diurnal cycle of the West African monsoon circulation. *Quarterly Journal of the Royal Meteorological Society,* 131**,** 2839-2860.

Peyrille, P. & Lafore, J. P. 2007. An idealized two-dimensional framework to study the West African monsoon. Part II: Large-scale advection and the diurnal cycle. *Journal of the Atmospheric Sciences,* 64**,** 2783-2803.

Randles, C. A., Kinne, S., Myhre, G., Schulz, M., Stier, P., Fischer, J., Doppler, L., Highwood, E., Ryder, C., Harris, B., Huttunen, J., Ma, Y., Pinker, R. T., Mayer, B., Neubauer, D., Hitzenberger, R., Oreopoulos, L., Lee, D., Pitari, G., Di Genova, G., Quaas, J., Rose, F. G., Kato, S., Rumbold, S. T., Vardavas, I., Hatzianastassiou, N., Matsoukas, C., Yu, H., Zhang, F., Zhang, H. & Lu, P. 2013. Intercomparison of shortwave radiative transfer schemes in global aerosol modeling: results from the AeroCom Radiative Transfer Experiment. *Atmospheric Chemistry and Physics,* 13**,** 2347-2379.

Ridley, D. A., Heald, C. L. & Ford, B. 2012. North African dust export and deposition: A satellite and model perspective. *Journal of Geophysical Research-Atmospheres,* 117.

Rienecker, M. M., Suarez, M. J., Gelaro, R., Todling, R., Bacmeister, J., Liu, E., Bosilovich, M. G., Schubert, S. D., Takacs, L., Kim, G. K., Bloom, S., Chen, J. Y., Collins, D., Conaty, A., Da Silva, A., Gu, W., Joiner, J., Koster, R. D., Lucchesi, R., Molod, A., Owens, T., Pawson, S., Pegion, P., Redder, C. R., Reichle, R., Robertson, F. R., Ruddick, A. G., Sienkiewicz, M. & Woollen, J. 2011. MERRA: NASA's Modern-Era Retrospective Analysis for Research and Applications. *Journal of Climate,* 24**,** 3624-3648.

Roberts, A. J., Marsham, J. H. & Knippertz, P. 2015. Disagreements in Low-Level Moisture between (Re)Analyses over Summertime West Africa. *Monthly Weather Review,* 143**,** 1193-1211.

Rocha-Lima, A., J. Vanderlei M. J., Remer, L. A., Todd, M., Marsham4, J. H., Engelstaedter, S., Ryder, C. L., Cavazos-Guerra, C., Artaxo, P., Colarco, P., Washington, R., A detailed characterization of the Saharan dust collected during the Fennec Campaign in 2011: in situ ground-based and laboratory measurements(submitted manuscript)

Roehrig, R., Bouniol, D., Guichard, F., Hourdin, F. & Redelsperger, J. L. 2013. The Present and Future of the West African Monsoon: A Process-Oriented Assessment of CMIP5 Simulations along the AMMA Transect. *Journal of Climate,* 26**,** 6471-6505.

Ryder, C. L., Highwood, E. J., Lai, T. M., Sodemann, H. & Marsham, J. H. 2013a. Impact of atmospheric transport on the evolution of microphysical and optical properties of Saharan dust. *Geophysical Research Letters,* 40**,** 2433-2438.

Ryder, C. L., Highwood, E. J., Rosenberg, P. D., Trembath, J., Brooke, J. K., Bart, M., Dean, A., Crosier, J., Dorsey, J., Brindley, H., Banks, J., Marsham, J. H., McQuaid, J. B., Sodemann, H. & Washington, R. 2013b. Optical properties of Saharan dust aerosol and contribution from the coarse mode as measured during the Fennec 2011 aircraft campaign. *Atmospheric Chemistry and Physics,* 13**,** 303-325.

Ryder, C. L., McQuaid, J. B., Flamant, C., Rosenberg, P. D., Washington, R., Brindley, H. E., Highwood, E. J., Marsham, J. H., Parker, D. J., Todd, M. C., Banks, J. R., Brooke, J. K., Engelstaedter, S., Estelles, V., Formenti, P., Garcia-Carreras, L., Kocha, C., Marenco, F., Sodemann, H., Allen, C. J. T., Bourdon, A., Bart, M., Cavazos-Guerra, C., Chevaillier, S., Crosier, J., Darbyshire, E., Dean, A. R., Dorsey, J. R., Kent, J., O'Sullivan, D., Schepanski, K., Szpek, K., Trembath, J. & Woolley, A. 2015. Advances in understanding mineral dust and boundary layer processes over the Sahara from Fennec aircraft observations. *Atmospheric Chemistry and Physics,* 15**,** 8479-8520.

Slingo, A., Ackerman, T. P., Allan, R. P., Kassianov, E. I., McFarlane, S. A., Robinson, G. J., Barnard, J. C., Miller, M. A., Harries, J. E., Russell, J. E. & Dewitte, S. 2006. Observations of the impact of a major Saharan dust storm on the atmospheric radiation balance. *Geophysical Research Letters,* 33.

Stein, T. H. M., Parker, D. J., Hogan, R. J., Birch, C. E., Holloway, C. E., Lister, G. M. S., Marsham, J. H. & Woolnough, S. J. 2015. The representation of the West African monsoon vertical cloud structure in the Met Office Unified Model: an evaluation with CloudSat. *Quarterly Journal of the Royal Meteorological Society,* 141**,** 3312-3324.

Sultan, B. & Janicot, S. 2003. The West African monsoon dynamics. Part II: The "preonset" and "onset" of the summer monsoon. *Journal of Climate,* 16**,** 3407-3427.

Thorncroft, C. D. & Blackburn, M. 1999. Maintenance of the African easterly jet. *Quarterly Journal of the Royal Meteorological Society,* 125**,** 763-786.

Todd, M. C., Allen, C. J. T., Bart, M., Bechir, M., Bentefouet, J., Brooks, B. J., Cavazos-Guerra, C., Clovis, T., Deyane, S., Dieh, M., Engelstaedter, S., Flamant, C., Garcia-Carreras, L., Gandega, A., Gascoyne, M., Hobby, M., Kocha, C., Lavaysse, C., Marsham, J. H., Martins, J. V., McQuaid, J. B., Ngamini, J. B., Parker, D. J., Podvin, T., Rocha-Lima, A., Traore, S., Wang, Y. & Washington, R. 2013. Meteorological and dust aerosol conditions over the western Saharan region observed at Fennec Supersite-2 during the intensive observation period in June 2011. *Journal of Geophysical Research-Atmospheres,* 118**,** 8426-8447.

Todd, M. C. & Cavazos-Guerra, C. 2016. Dust aerosol emission over the Sahara during summertime from Cloud-Aerosol Lidar with Orthogonal Polarization (CALIOP) observations. *Atmospheric Environment,* 128**,** 147-157.

Trzeciak, T. M., Garcia-Carreras, L. & Marsham, J. H. 2017. Cross-Saharan transport of water vapor via recycled cold pool outflows from moist convection. *Geophysical Research Letters,* 44**,** 1554-1563.

Wielicki, B. A. 1996. Clouds and the Earth's radiant energy system (CERES): An earth observing system experiment (vol 77, pg 860, 1996). *Bulletin of the American Meteorological Society,* 77**,** 1590-1590.

Winker, D. M., Vaughan, M. A., Omar, A., Hu, Y. X., Powell, K. A., Liu, Z. Y., Hunt, W. H. & Young, S. A. 2009. Overview of the CALIPSO Mission and CALIOP Data Processing Algorithms. *Journal of Atmospheric and Oceanic Technology,* 26**,** 2310-2323.

Xue, Y. K., De Sales, F., Lau, W. K. M., Boone, A., Feng, J. M., Dirmeyer, P., Guo, Z. C., Kim, K. M., Kitoh, A., Kumar, V., Poccard-Leclercq, I., Mahowald, N., Moufouma-Okia, W., Pegion, P., Rowell, D. P., Schemm, J., Schubert, S. D., Sealy, A., Thiaw, W. M., Vintzileos, A., Williams, S. F. & Wu, M. L. C. 2010. Intercomparison and analyses of the climatology of the West African Monsoon in the West African Monsoon Modeling and Evaluation project (WAMME) first model intercomparison experiment. *Climate Dynamics,* 35**,** 3-27.

Yang, E. S., Gupta, P. & Christopher, S. A. 2009. Net radiative effect of dust aerosols from satellite measurements over Sahara. *Geophysical Research Letters,* 36.

Figure Captions

Figure 1. Climatological state of the Saharan heat Low region (mean of June, ~~JJAS from~~ 1979-2013): SHL location, low level circulation, and dust load. Shaded: the mean position of heat low region (occurrence frequency of 90% of llat), arrows: mean 925 hPa wind, Blue Line: the mean position of the inter-tropical discontinuity from ERA-Int reanalysis data and aerosol optical depth (AOD) from satellite MISR data (contour intervals are 0.4, 0.6, and 0.8 for grey, white, and cyan lines). The purple rectangle denotes location of the FENNEC Supersite 1 (SS1)

Figure 2. Vertical Profile Specific Humidity (g kg^{-1}) (a) FENNEC radiosonde measurements (b) ERA-INT and (c) Difference between (a) and (b). Red arrows in (a) denote times of major haboob events

Figure 3. Diurnal Cycle of mean Surface Albedo at BBM

Figure 4~~6~~. Surface skin temperature (SKT) (stars), and 2 m air temperature (diamonds) at BBM. ~~: Skin Temperature Black: ERAI, Red: MERRA, and Green Star: CERES footprint, 2 m air temperature Gold: ERAI and Cyan: Flux Tower measurement.~~ The bigger black and red stars denote ERAI and MERRA skin temperature at the time steps when there is CERES observation.

Figure 5~~7~~. Wavelength dependence of optical properties of dust particle for longwave (a, b, c) and shortwave (d, e, f). (a) and (d) mass extinction coefficient, (b) and (e) single scattering albedo, and (c) and (f) asymmetry parameter. ~~(top three panel) and shortwave (bottom three panel).~~ The continuous lines are the spectrally resolved optical properties and the horizontal lines are the band-averaged data that are used in the RT code.

Figure 6~~4~~. CALIOP~~Caliop~~ mean Extinction Coefficient profile at BBM 2006-13

Figure 7. AOD from AERONET and SEVIRI, and column integrated water vapour from FENNEC observation. Gray shades show driest days (11, 12, and 16), blue shades shows most humid days (18, 25, and 30), and green shade shows a major haboob event occurred on the 21th which resulted in large dust emission.

~~**Figure 5**. AOD from AERONET and SEVIRI, and column integrated water vapour from FENNEC observation. Gray shades show driest (11, 12, and 16), blue shades shows most humid days (18, 25, and 30) Nephelometer measurement and green shade shows a major haboob event occurred on the 21th which resulted in large dust emission~~

~~**Figure 6**. Surface skin temperature (SKT) and 2-m air temperature at BBM: Skin Temperature Black: ERAI, Red: MERRA, and Green Star: CERES footprint, 2-m air temperature Cold:ERAI and Cyan: Flux Tower measurement. The black and red stars denote ERAI and MERRA skin temperature at the time steps when there is CERES observation.~~

~~**Figure 7**. Wavelength dependence of optical properties of dust particle for longwave (top three panel) and shortwave (bottom three panel). The continuous lines are the spectrally resolved optical properties and the horizontal lines are the band-averaged data that are used in the RT code.~~

Figure 8. Mean Diurnal Cycle of TOA Flux. (a) shortwave and (b) longwave. ~~Blue:~~ SOCRATES results are from wDwC experiment. ~~and green: GERB~~

Figure 9. Time series of Radiative Flux at BBM. TOA- longwave (a), shortwave (b), and net (c). S~~(left column) and S~~urface ~~(right column)~~ shortwave (d), ~~(SW)~~ , longwave (e), and net (f) ~~longwave (LW), and net Radiative Flux at BBM~~. ~~Black lines denote SOCRATES outputs, red line denote GERB measurements, green dots denote CERES measurements~~The bigger ~~and~~ red dots denote GERB measurements corresponding to CERES time steps.

Figure 10. Mean d~~D~~iurnal direct radiative effect of dust averaged for June 08-30, 2011~~6~~. (a) TOA ~~DRE of Dust (a)~~ and (b) s~~S~~urface ~~DRE of Dust (b)~~. The bars show standard error over the diurnal cycle.

~~**Figure 11**. DRE due to Dust: time series of TOA shortwave (a), longwave (b), net (c) and surface shortwave (d) longwave (e) and net (f) wdnC-nDnC flux~~

Figure 1~~2~~1 Radiative budget as a function of dust AOD. Top row (a, b, c): TOA -longwave (a), shortwave (b), and net (c). Second row (d, e, f): similar to top row but for surface. Third Row: atmospheric radiative convergence of longwave (g), shortwave (g), and net (i).

Figure 1~~2~~3. Mean r~~R~~adiative h~~H~~eating Rate Profile for June (08-30, 2011) at BBM. (a)~~:~~ Results from nDnC (dashed lines) and wDnC (solid lines) using FENEC profile and (b)~~:~~ MERRA Model output for all sky (solid lines) and clear sky (dashed lines) conditions. ~~Blue, red, and green colours represent shortwave, longwave, and total heating rates respectively.~~

Figure 1~~3~~4 Shortwave r~~R~~adiative h~~H~~eating rates (K.Day^{-1}) of dust in the atmosphere (~~DUST represents~~ wDnC ~~runs~~ minus~~and CLEAN represents~~ nDnC ~~runs~~)

Figure 1~~4~~5 Atmospheric h~~H~~eating rate profile for selected dry days, June 11, 12, and 16 (dashed lines) and moist days, June 18, 19, and 25 (solid lines)

Figure 1~~5~~6 Same as ~~Figure~~Fig. 1~~1~~2 except for column integrated water vapour.

Figure 1~~6~~7 Sensitivity of Radiative Flux (W.m^{-2}) to changes in dust AOD ~~and column integrated water vapour~~. The numbers at each pressure level are downward shortwave (blue), longwave (red), and net (green) flux. The grey shade represents dust and water vapour amount in the atmosphere

Figure 17 Same as Fig. 16 except for changes in column integrated water vapour

Formatted: Left, Don't add space between paragraphs of the same style

Formatted: Font: Bold

Tables

Table 1. Summary of model configuration mode sensitivity analysis

Sensitivity input variable	Source of data for sensitivity run	Sensitivity results	'Optimal configuration choice

surface albedo	Fennec measured quantity versus ERA-I	Difference of upto 16 W.m^{-2} in TOA net SW flux	Surface Albedo calculated from surface flux measurements
skin temperature	ERA-I MERRA	Difference of 6 W.m^{-2} in surface net LW flux	ERA-I skin temperature estimate
Surface emissivity	CERES MERRA	Differences of 2.3 W.m^{-2} at TOA LW flux and 5 W.m^{-2} at the surface.	MERRA reanalysis estimates
Cloud fraction and mixing ratio	ERA-I MERRA	Difference of 4 W.m^{-2} both at TOA and surface net SW flux	ERA-I
dust size distribution	Dubovik FENNEC-Ryder	TOA SW dust DRE -2 w.m^{-2} Using Dubovik and 23 w.m^{-2} using Ryder-FENNEC	Dubovik

Formatted Table

Table 12. Description of the RT 'experiment mode'. Names of different experiments acronyms are defined as 'n' = NO, 'w' = with, 'D' = Dust, 'C' = Cloud, 'WV' = water vapour, and 'sen' = sensitivity

Name	Description	Water vapour	Aerosol	Cloud
nDnC	Dust free and Cloud free atmosphere	Observed 8th-30th June 2011	None	None
nDwC	Dust free but cloudy atmosphere	Observed 8th-30th June 2011 diurnal cycle	None	ERAI MERRA
wDnC	Cloud free but dusty atmosphere	Observed 8th-30th June 2011 diurnal cycle	AERONET AOD scaled with CALIOP Extinction	None
wDwC	Dusty and Cloudy Atmosphere	Observed 8th-30th June 2011 diurnal cycle	AERONET AOD scaled with CALIOP Extinction	ERAI MERRA
senDnC	Sensitivity to full range of possible AOD	Mean diurnal WV	Linear increase in AOD 0.0 to 3.0 Constant AOD each time step for a given run	None

senWVwDnC	Sensitivity to full range of possible WV	Linear increase in TCWV from 10 to 40kg.m-2 at 2.5 kg.m^{-2}interval with mean diurnal WV profile	Mean Diurnal AOD	None

Table ~~3~~2. Mean June 08-30, 2011 TOA Radiative flux at BBM (definition of acronyms are given in table 2). Values are in W.m^{-2}. The sign convention is that downward flux is considered as positive while upward flux is negative. On column 6 red (blue) fonts indicate model results overestimated (underestimated) compared with observation.

		nDnC	nDwC	wDnC	wDwC
TOA_SW	SOCRATES	328	322	325	**321**
	GERB	--	--	--	**314**
	MERRA	312	307	322	**317**
	ERAI	--	--	336	**324**
TOA_LW	SOCRATES	-313	-304	-297	**-290**
	GERB	--	--	--	**-276**
	MERRA	-314	--	-307	**-296**
	ERAI	--	--	-309	**-294**
TOA_NET	SOCRATES	15	18	28	**31**
	GERB	--	--	--	**38**
	MERRA	-2	--	15	**20**
	ERAI	--	--	27	**29**

Table 34. Same as Table 3 but for surface radiative flux and observation from fennec instrument

		nDnC	nDwC	wDnC	wDwC
SRF_SW	SOCRATES	237	232	192	**187**
	FENNEC_OBS	--	--	--	**180**
	MERRA	220	215	190	**185**
	ERAI	--	--	210	**199**
SRF_LW	SOCRATES	-138	-134	-106	**-103**

Formatted: Font color: Red
Formatted: Font color: Red
Formatted: Font color: Red
Formatted: Font color: Red
Formatted: Font color: Light Blue
Formatted: Font color: Light Blue
Formatted: Font color: Red
Formatted: Font color: Red
Formatted: Font color: Red

	FENNEC_OBS	--	--	--	**-78**
	MERRA	-139	--	-119	**-115**
	ERAI	--	--	-139	**-132**
SRF_NET	SOCRATES	99	98	86	**84**
	FENNEC_OBS	--	--	--	**103**
	MERRA	82	--	70	**70**
	ERAI	--	--	71	**67**

Formatted: Font color: Red

Formatted: Font color: Light Blue

Formatted: Font color: Light Blue

~~**Table 45**. TOA and Surface Direct Radiative Effect of Dust and Cloud~~

	~~Dust DRE SOCRATES~~			~~Cloud DRE SOCRATES~~			~~Cloud DRE EBFA-CERES EBFA~~		
	~~SW~~	~~LW~~	~~NET~~	~~SW~~	~~LW~~	~~NET~~	~~SW~~	~~LW~~	~~NET~~
~~TOA~~	~~-3~~	~~16~~	~~13~~	~~-4~~	~~7~~	~~3~~	~~-15~~	~~16~~	~~1~~
~~SURFACE~~	~~-45~~	~~32~~	~~-13~~	~~-5~~	~~3~~	~~-2~~	~~-19~~	~~11~~	~~-8~~

Formatted: Centered

Formatted: Centered

Formatted: Centered

Formatted: Centered

Table ~~45~~6. Sensitivity of Radiative Flux to Dust AOD and CIWV at selected altitudes.
SD*=Standard Deviation (0.8 for AOD and 5.5 g.kg^{-1} for water vapour. Mean AOD = 1.2 and mean column integrated water vapour = 27.8 Kg.m^{-2})

Change in Flux		SW	LW	NET
per unit AOD (W.m^{-2})	TOA	-1.8	10.0	8.2
	Surface	-33.8	19.8	-14.0
	Convergence	32.1	-9.7	22.4
per unit CIWV (W.Kg^{-1})	TOA	0.3	1.1	1.4
	Surface	-0.4	1.6	1.2
	Convergence	0.8~~7~~	-0.5~~6~~	0.3~~1~~
per one AOD SD* (W.m^{-2})	TOA	-1.4	8.0	6.6
	500hPa	-6.2	10.6	4.4
	700hPa	-14.8	11.6	-3.2
	Surface	-27.0	15.8	-11.3
	Convergence	25.7	-7.8	17.9
per one CIWV SD* (W.Kg^{-1})	TOA	1.7	5.8	7.5
	500hPa	-0.4	9.3	8.9

Formatted Table

700hPa	-1.6	9.4	7.9
Surface	-2.4	8.3	5.9
Convergence	4.0	-2.8	1.3

Figures

Formatted: Indent: First line: 0 cm

Formatted: Justified, Add space between paragraphs of the same style

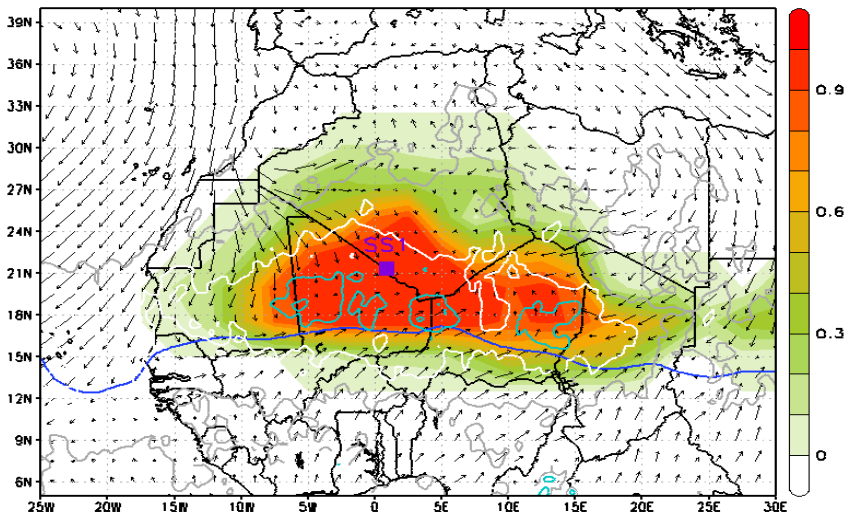

~~Figures~~

Formatted: Indent: First line: 0 cm

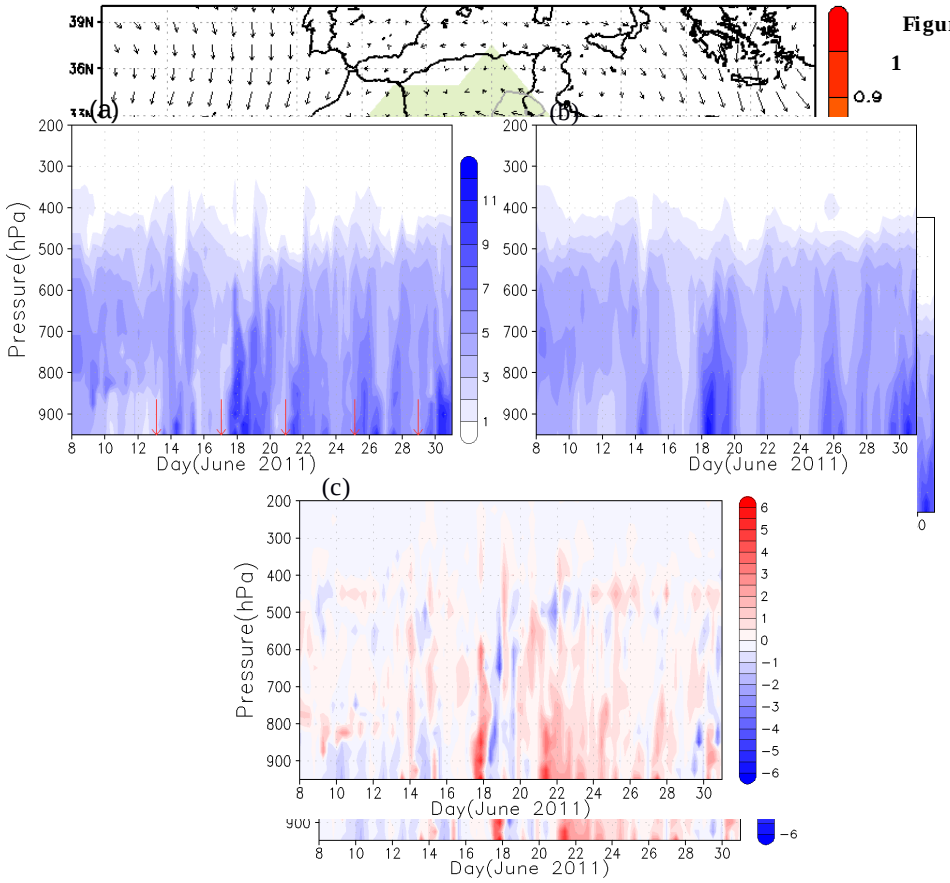

Figure 1

Formatted: Justified, Add space between paragraphs of the same style

Figure 2

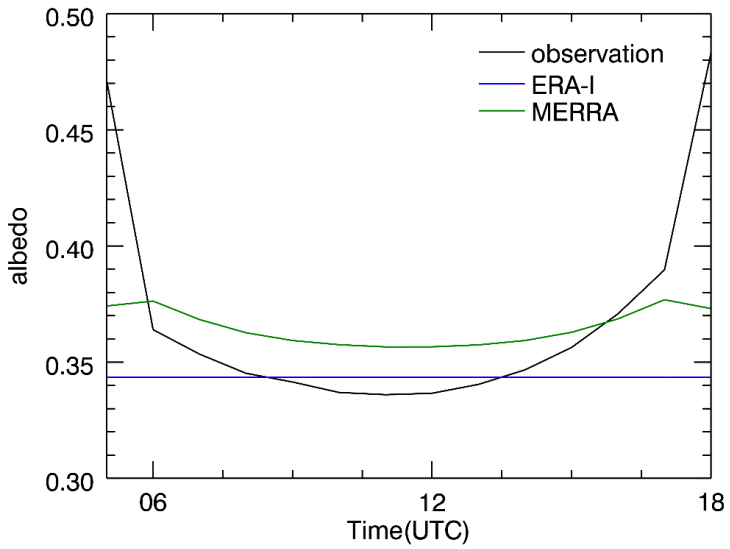
0.50
0.45
0.40
0.35
0.30
albedo
06
12
18
Time(UTC)
observation
ERA-I
MERRA

Figure 3

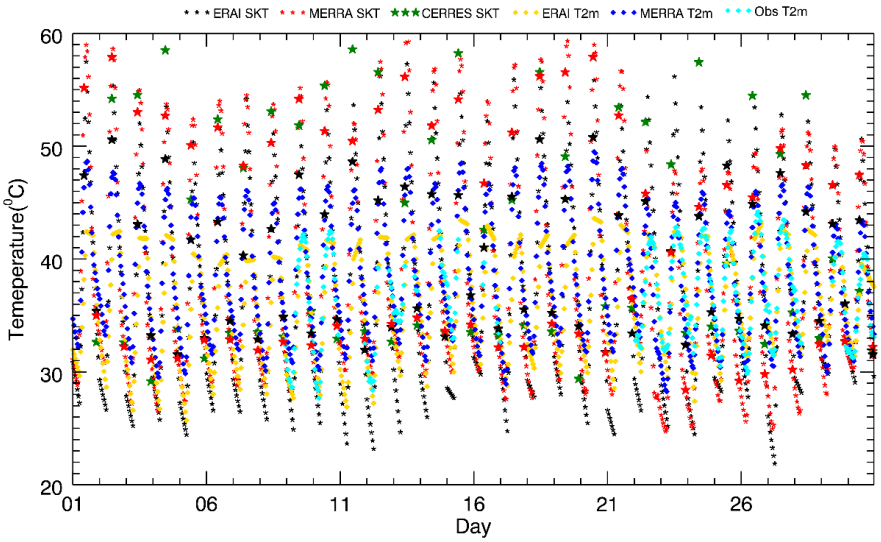

Figure 4

Formatted: Font: Bold

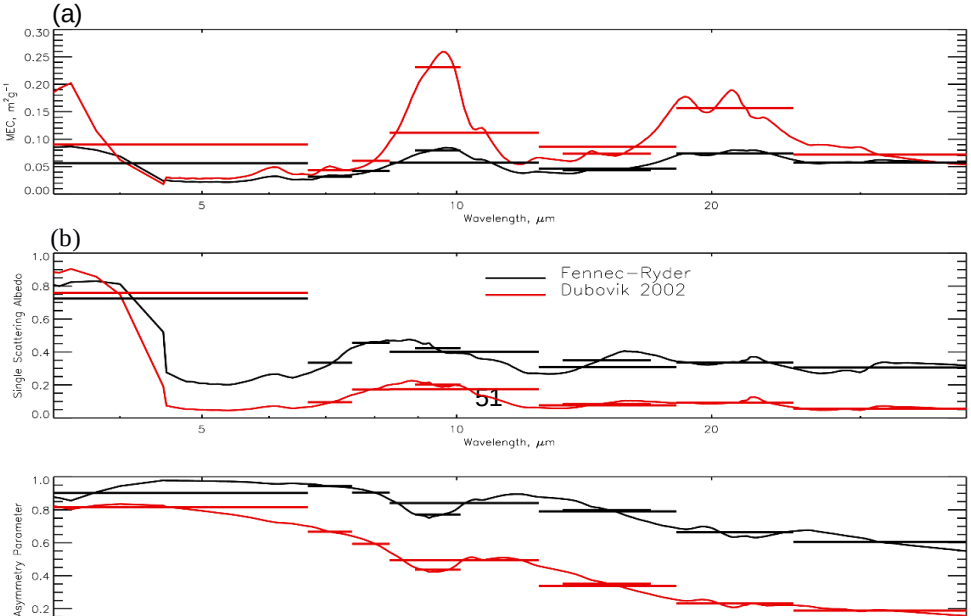

Figure 5

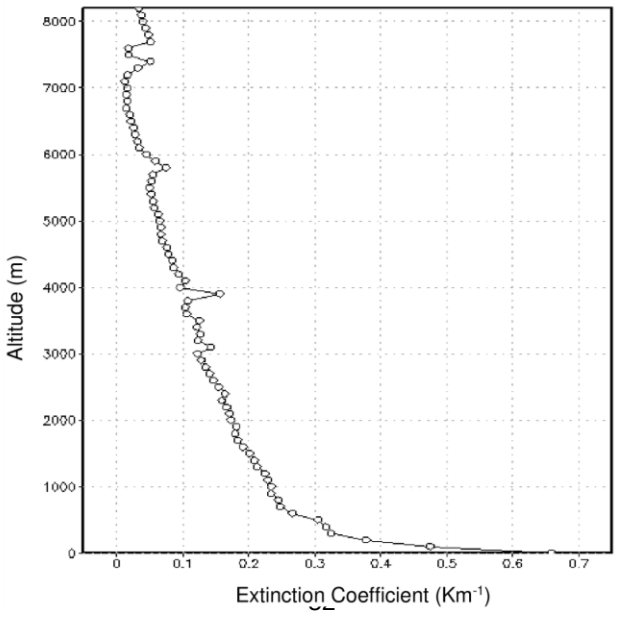
Altitude (m)
8000
7000
6000
5000
4000
3000
2000
1000
0
0
0.1
0.2
0.3
0.4
0.5
0.6
0.7
Extinction Coefficient (Km-1)

Figure 6

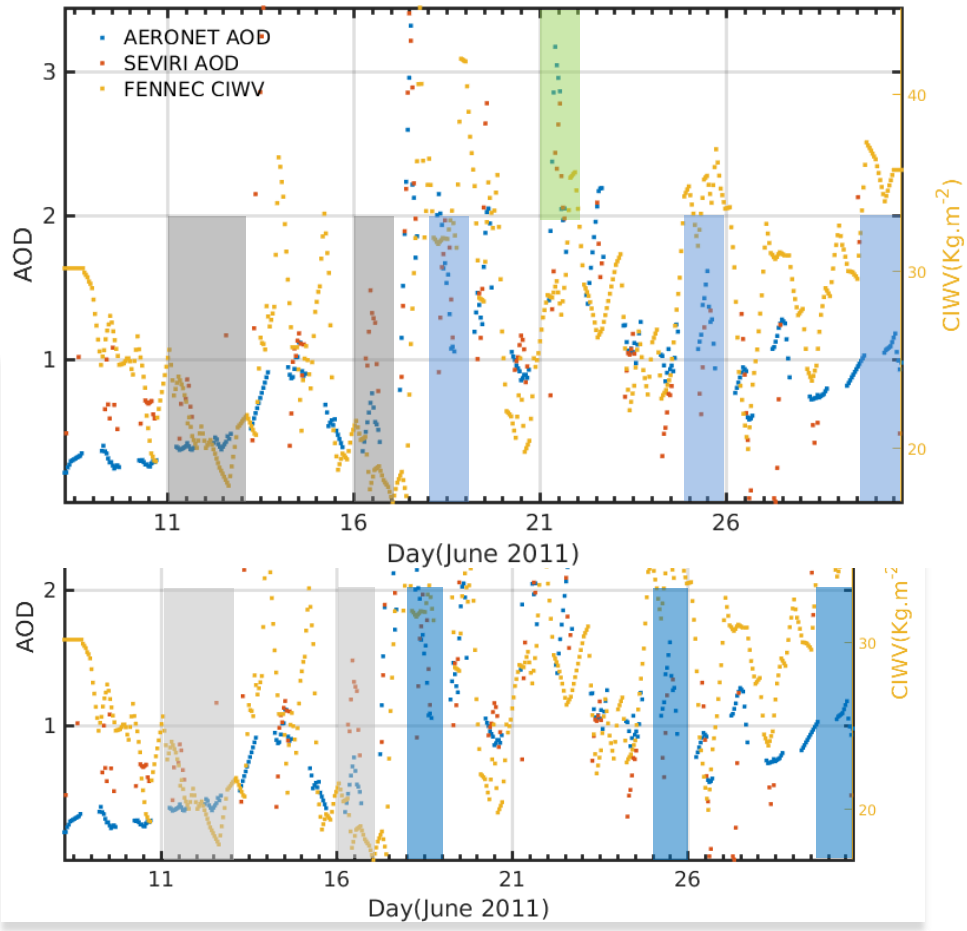
AERONET AOD
SEVIRI AOD
FENNEC CIWV
AOD
CIWV(Kg.m-2)
Day(June 2011)
11
16
21
26
1
2
3
20
30
40

Figure 7

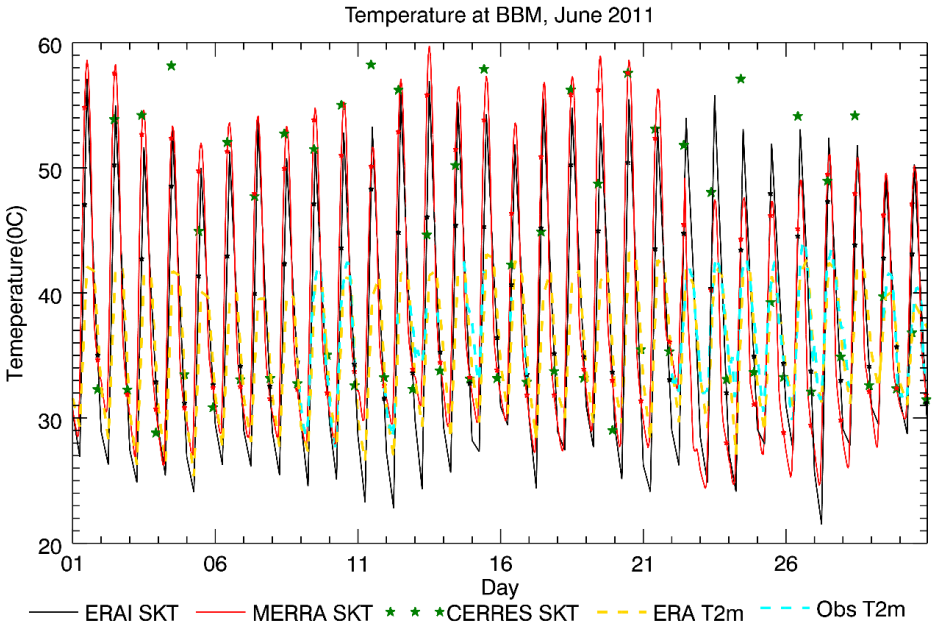
Temperature at BBM, June 2011
Temeperature(0C)
60
50
40
30
20
01
06
11
16
21
26
Day
ERAI SKT
MERRA SKT
CERRES SKT
ERA T2m
Obs T2m

~~Figure 6~~

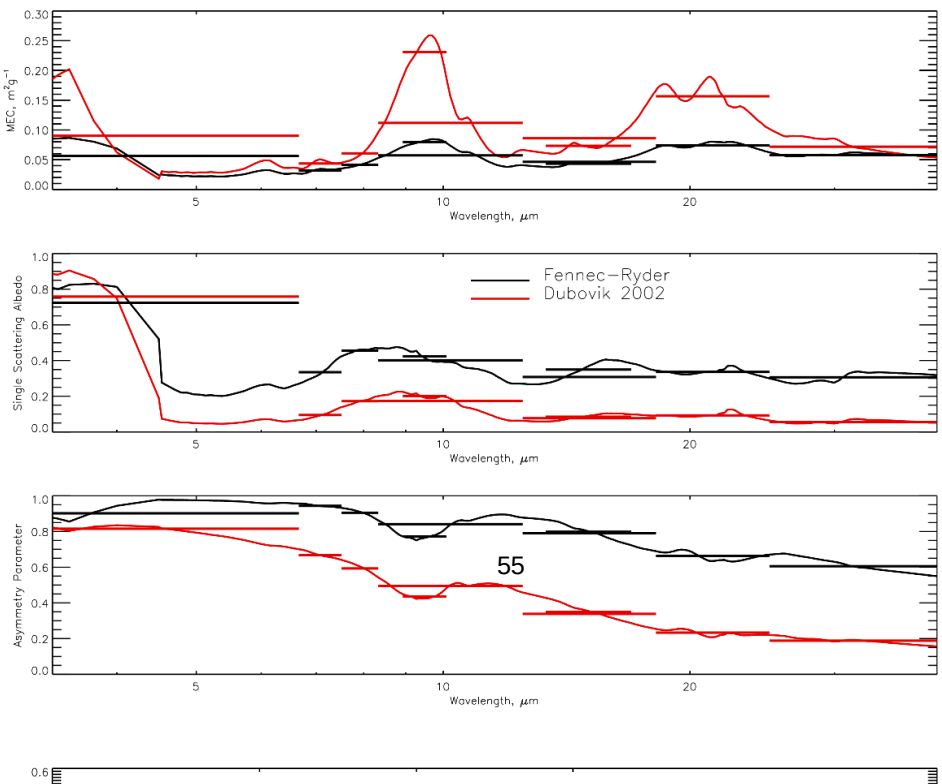
MEC, m²g⁻¹
0.30
0.25
0.20
0.15
0.10
0.05
0.00
5
10
20
Wavelength, μm
Single Scattering Albedo
1.0
0.8
0.6
0.4
0.2
0.0
Fennec–Ryder
Dubovik 2002
5
10
20
Wavelength, μm
Asymmetry Parameter
1.0
0.8
0.6
0.4
0.2
0.0
5
10
20
Wavelength, μm
0.6

Figure 7

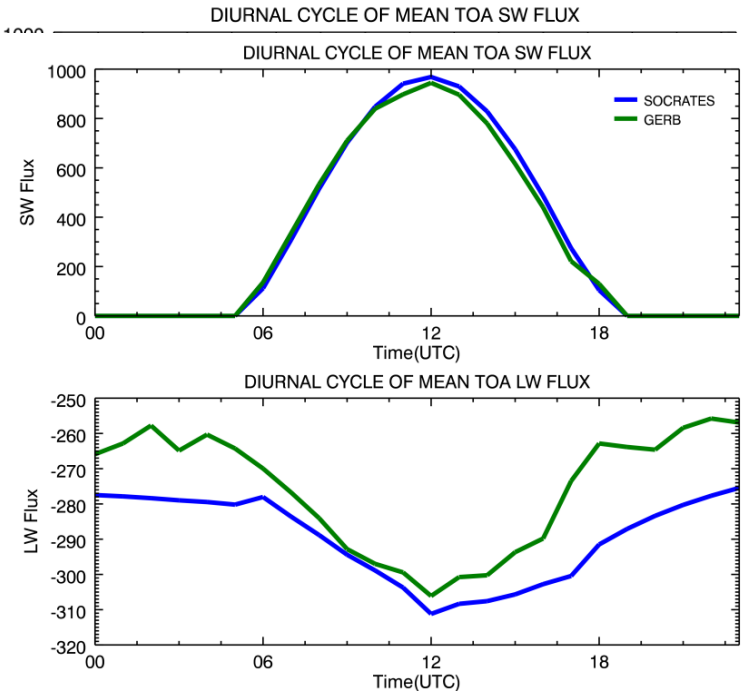
DIURNAL CYCLE OF MEAN TOA SW FLUX
DIURNAL CYCLE OF MEAN TOA SW FLUX
SOCRATES
GERB
SW Flux
1000
800
600
400
200
0
00
06
12
18
Time(UTC)
DIURNAL CYCLE OF MEAN TOA LW FLUX
LW Flux
-250
-260
-270
-280
-290
-300
-310
-320
00
06
12
18
Time(UTC)

Figure 8

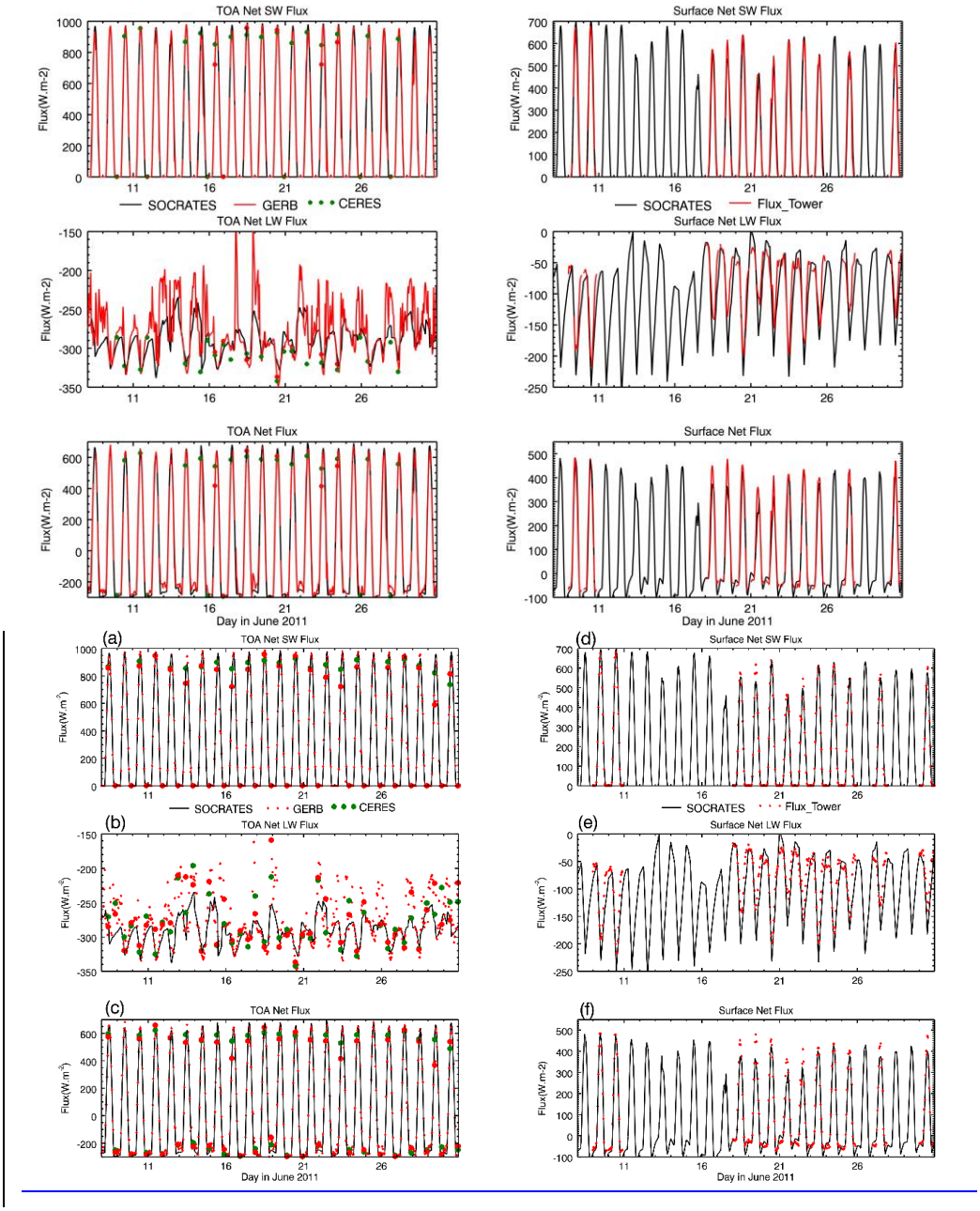
TOA Net SW Flux
Surface Net SW Flux
Flux(W.m-2)
SOCRATES
GERB
CERES
Flux_Tower
TOA Net LW Flux
Surface Net LW Flux
TOA Net Flux
Surface Net Flux
Day in June 2011
(a)
(b)
(c)
(d)
(e)
(f)
Flux(W.m-2)

Figure 9

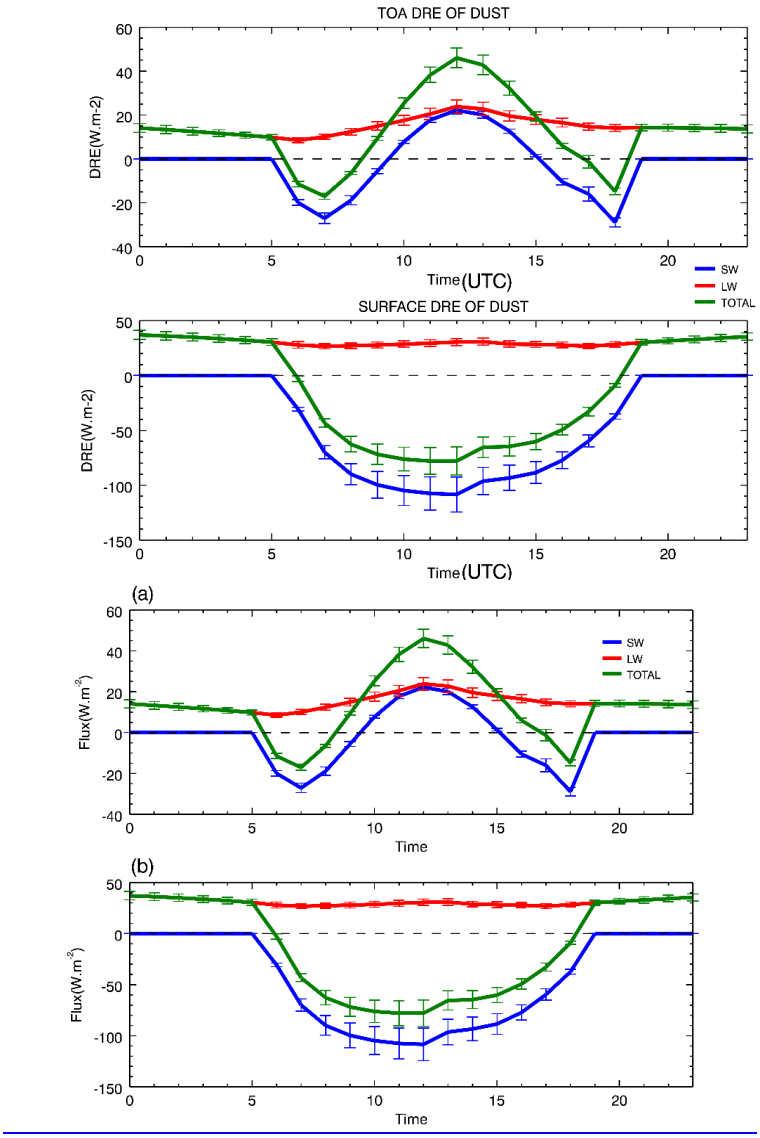
TOA DRE OF DUST
DRE(W.m-2)
Time(UTC)
SW
LW
TOTAL
SURFACE DRE OF DUST
DRE(W.m-2)
Time(UTC)
(a)
Flux(W.m-2)
Time
(b)
Flux(W.m-2)
Time

Figure 10

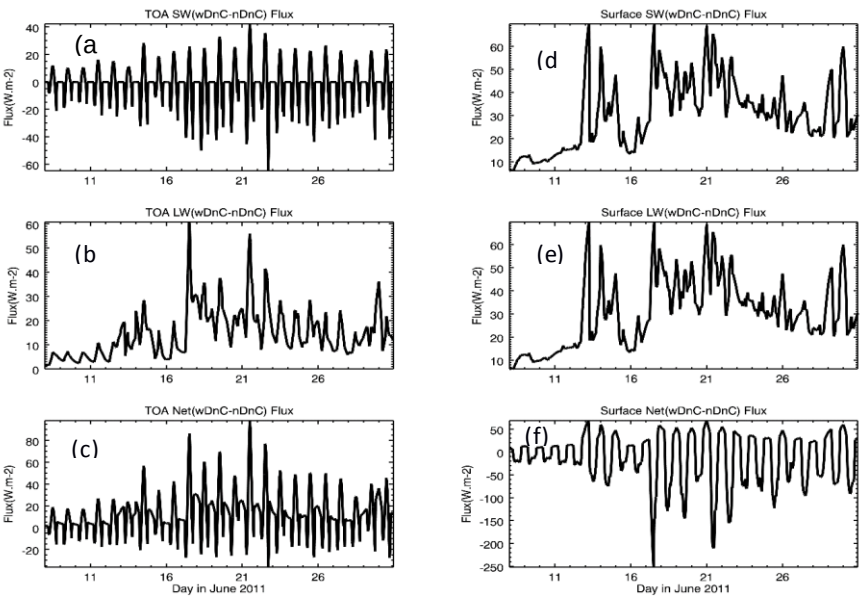
TOA SW(wDnC-nDnC) Flux
(a)
Surface SW(wDnC-nDnC) Flux
(d)
TOA LW(wDnC-nDnC) Flux
(b)
Surface LW(wDnC-nDnC) Flux
(e)
TOA Net(wDnC-nDnC) Flux
(c)
Surface Net(wDnC-nDnC) Flux
(f)
Flux(W.m-2)
Day in June 2011

~~Figure 11~~

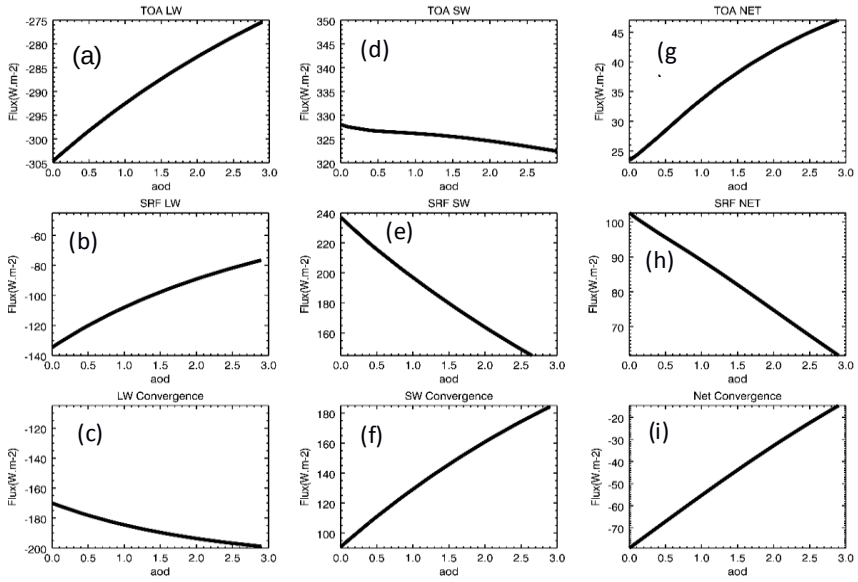

Figure 1[1]

~~2~~

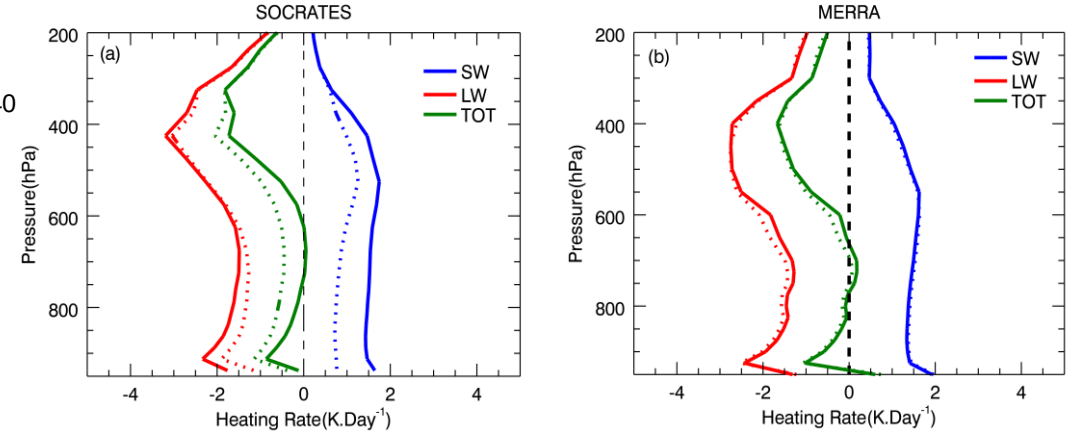

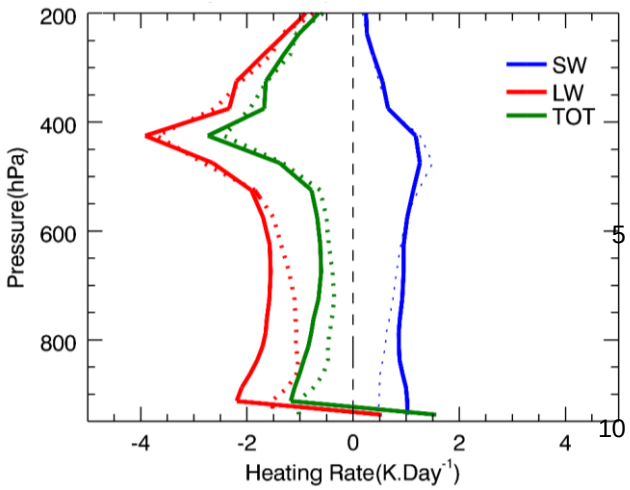

Figure 13

Figure 123

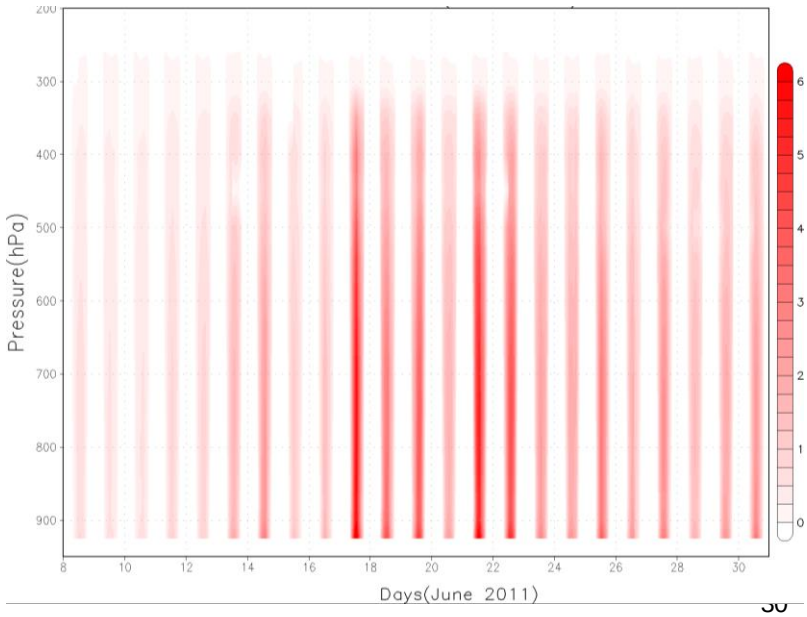

Formatted: French (France)

Figure 134

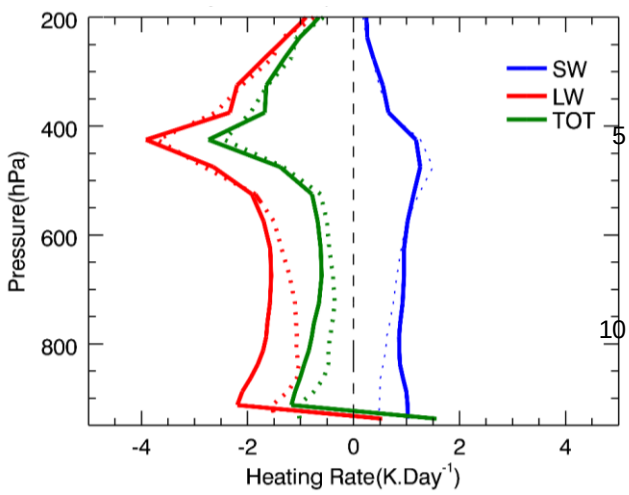

Figure 14

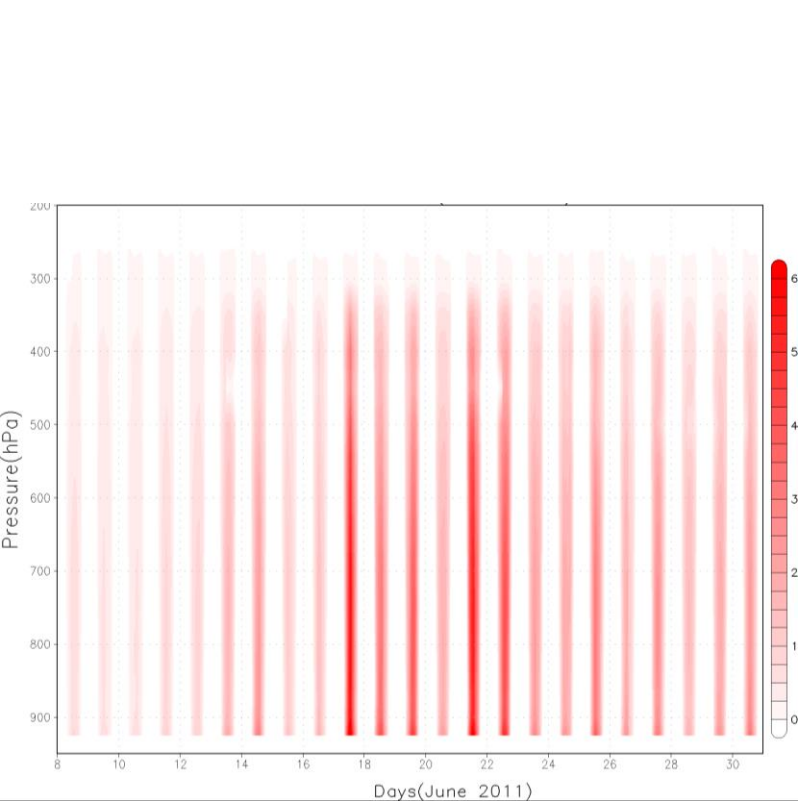

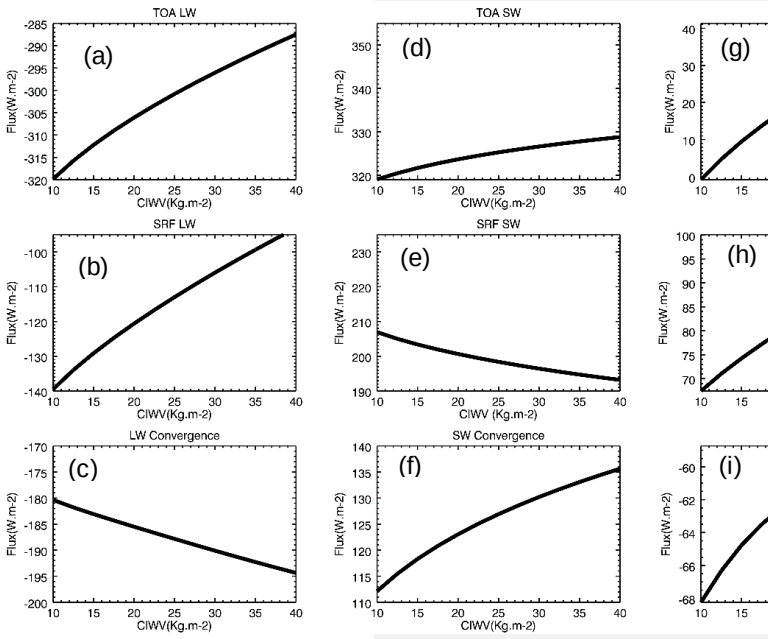

Figure 15

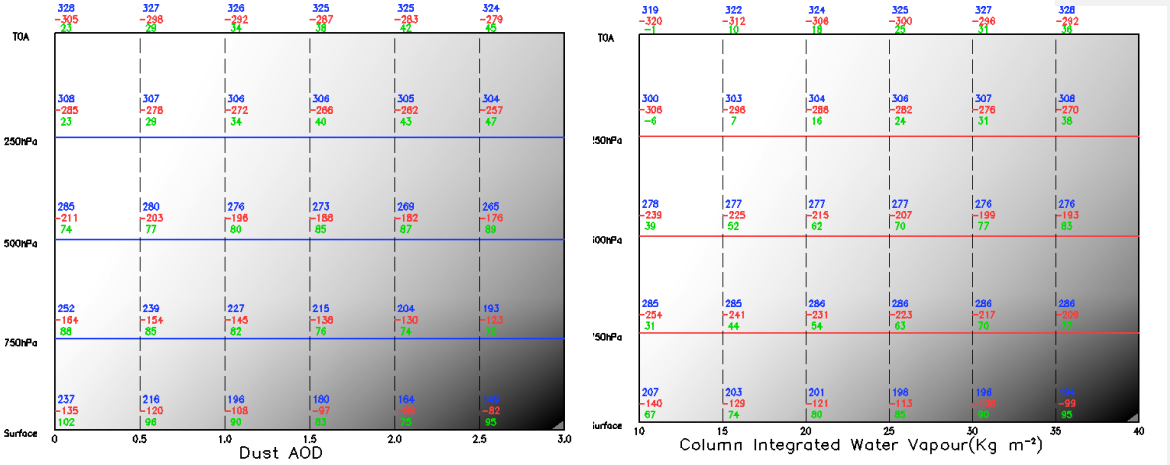

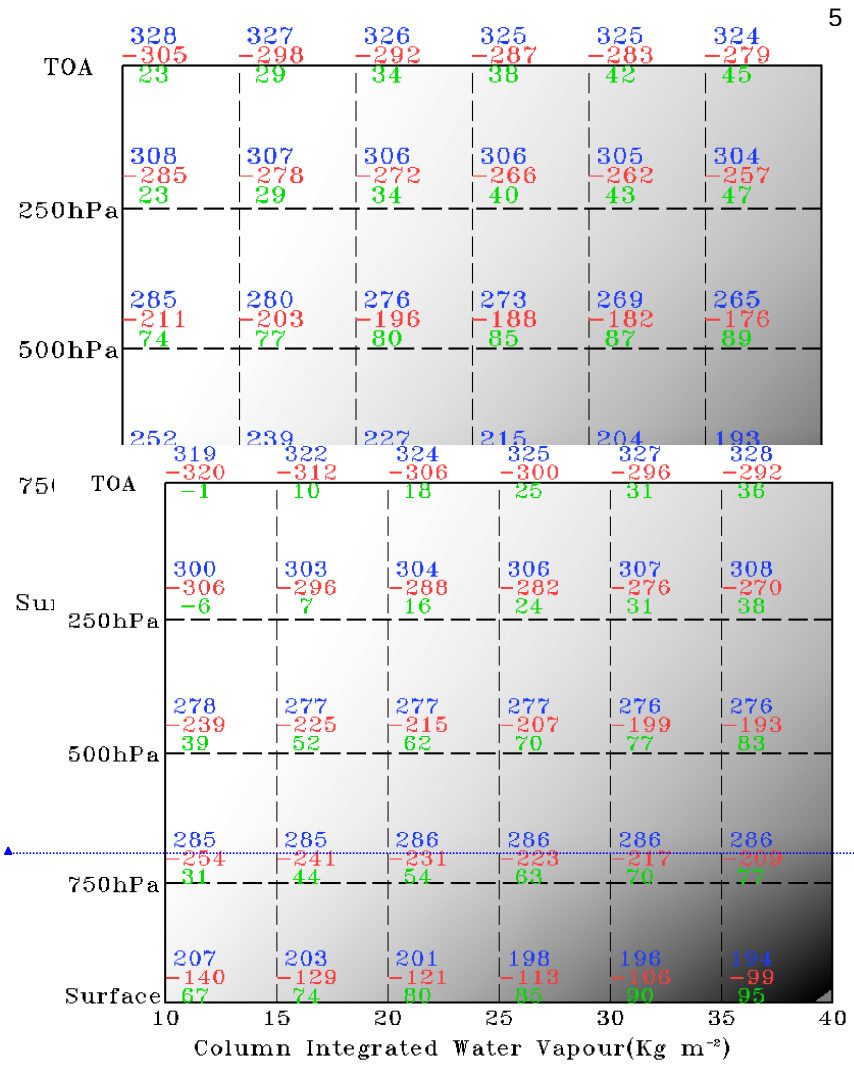

Figure 16

Formatted: Font: (Default) Times New Roman, 10 pt, Bold, Complex Script Font: Times New Roman, 10 pt

Formatted: Font: (Default) Times New Roman, 10 pt, Bold, Complex Script Font: Times New Roman, 10 pt

Figure 17

Formatted: Font: (Default) Times New Roman, 10 pt, Bold, Complex Script Font: Times New Roman, 10 pt

Formatted: Font: (Default) Times New Roman, 10 pt, Complex Script Font: Times New Roman, 10 pt

'The summertime Saharan heat low: Sensitivity of the radiation budget and atmospheric heating to water vapour and dust aerosol' by Netsanet K. Alamirew et al

The comments and suggestions made by all referees and reviewer are useful. We have addressed the comments raised. Our responses and changes (if any) are indicated in the corrected version of the paper. For clarity we put original comment of the reviewer (typed in italic font) followed by our responses to make it easy to follow.

Response to interactive discussion Short Comment (SC) from C. Lavaysse

Major Comment a.

1. *Section 3 is not clear. Quite complicated to understand all the configurations and the conclusions drawn from these results on the choice of certain parameters. Finally choices are not really justified and I am not sure if it is necessary to provide all the information. I would recommend to simplify this section and to put some results in the supplementary material.*

Response

Part of section 3 has been moved to the supplementary material (Section S2). This includes all the model configuration analysis. Accordingly, Section 3 now describes the data and the design of the hypothesis testing experiments and Section 4 focuses only on the results of those experiments.

Changes Made

We have reorganized section 2 and 3 into a more clear structure. The new structure of the whole paper is as follows.

Section 1. Introduction
Section 2. Description of RT model
Section 3. Data and method
- 3.1. Observed top of atmosphere and surface radiation measurements
- 3.2. Atmospheric profile and surface characteristics
- 3.3. Dust properties and extinction profile
- 3.4. RT model Experiments

Section 4. Results and discussions.
- 4.1. RT model validation
- 4.2. The radiative flux and heating effects of dust and water vapour
  - 4.2.1. Dust
  - 4.2.2. Water vapour
  - 4.2.3. The relative effects of dust versus water vapour

Section 5. Summary and Conclusions

Original draft Page 6:L19-40, Page 7:L1-3, Page 7:L28-37 moved to supplementary material (section S2). See also minor comment #3.

2. *In this section I also found some parts not clear: p5 l5-12; it is quite weird to compare observations assimilated with model dataset? The authors do not explain the remaining errors. Is it due to the assimilation procedure?*

Response

We are pointing the fact that despite assimilation of the radiosonde data there remain biases in the reanalysis. Fennec was a short-term experiment and since then there remains only one radiosonde station for the whole Sahara. As such, the reanalysis errors we derive are almost certainly much lower than those typical of the rest of the Sahara. We also now cite the errors estimated from Garcia-Carreras who compared radiosonde data to a forecast model first guess (independent of assimilation)

The magnitude of errors are different among the different reanalysis products. The possible reasons for the remaining error between observation and reanalysis products could be due to differences in models core dynamics and in assimilation procedures.

Changes Made

Corrected draft Page 4. L36-38. A statement added suggesting the possible reasons for differences in error among reanalyses.

Major Comment b.

1. *Section 4 is too descriptive with too much information that are not necessarily significant or important to the conclusions of this study. This is particularly true p9 and 10. I strongly recommend to reduce this part to the most important results and to put the others results into an annex.*

Response

Part of section 4 has been moved to the supplementary Material (section S3), specifically sections describing the sensitivity experiments towards the model optimum configuration, as we agree these are not the key significant results.

We choose to retain some of the results originally presented in pages 9-10 because we feel it is important to demonstrate that the simulated quantities of top of atmosphere radiation budgets are within the observational uncertainties. To give sense of results in subsequent sections, it is necessary to have a feeling of the surface and TOA radiative budget under the mean state.

Changes Made

Original draft page 8:L30-33, page 9:L3-8 moved to supplementary material (section S3)

2. *The summary of the subsection 4.1 is too speculative. How the authors can conclude the simulated flux errors of the optimal configuration are comparable to the observational uncertainties? What does 'acceptable' mean?*

Response

Given that we do not have accurate data for all the input required to run the RT model, it is not unexpected to get some uncertainty in our results. However we have chosen the inputs in such a way that the calculated flux are as close as possible to observation. This is what we mean by an 'optimum' model configuration. The optimum configuration is deemed to be 'acceptable' because the model error in top of atmosphere fluxes (perhaps the single most important quantity) with respect to observations is within the uncertainty in the observational estimates of those quantities. Model estimates lying within observation range is a commonly used indicator of acceptable model performance. Thus we suggested the RT model is configured to produce acceptable results and thus can be used for further experiments.

Major Comment c.

1. *Some conclusions are too speculative. The authors conclude about the impacts of the dust aerosols and water vapor on the SHL but, in that study, only June 2011 is used. The SHL is the most important from end of June to mid of September (when it is installed in its Saharan location). Even if the authors used only one month (June), they have to characterize this specific year to the climatology (in term of dust, humidity, large scale forcings). This point concerns the title ('summertime' is not appropriate), the conclusions (p15 l8-10), and the abstract.*

Response

We agree that the period of study does not coincide with the peak of the summer season when the SHL is established in its northernmost position. However, we are limited by the period of the Fennec field campaign whose data underpin our analysis. Accordingly we have changed all references to 'summertime' to 'early summer'. In addition, in Section 3.2 we note that during our study period of June 2011 the SHL underwent a rapid transition from a 'maritime phase' to a 'heat low' phase. As such our analysis actually covers the transition period and SH states characteristic of both early and high summer. We have now amended this section to include an analysis of the conditions during June 2011 with respect to the mean conditions during June.

Changes Made

References to summer changed to summertime.
Figure 1 changed to show position of SHL in June, 2011.
Corrected draft Page 16:L14-20. A paragraph added

2. *Also the discussion on the impacts on the SHL pulsations should be carefully discussed since the authors do not analyze the contribution of the large scale temperature advections and they never show the real position of the SHL in June 2011 (in June, the SHL is migrating to the north with a large spatial variability).*

Response

Real position of SHL in June is shown in Fig 1.

The comments on our reference to variability in SHL specifically the 'pulsating' of SHL intensity and the potential role of dust and water vapour feedbacks in this process is also raised by anonymous referee #1. We do feel it is important in this paper to relate the radiative heating rates derived from our RT simulations to the behaviour of the SHL, but of course recognise that the full dynamical response requires an analysis of advective heating. As such in the original paper p16 para 1 we note that radiative heating is of 'comparable magnitude' to published estimates of advective cooling from comparable monsoon surge type events. In this way we make only a broad inference about the net effects of advective and radiative terms on the SHL. We have now changed the text slightly to emphasise the speculative nature of this inference.

Changes Made

Corrected draft Page 15:L26-28. Additional statement included.

'

3. *Finally at climatological scale, the authors should pay attention to the climatological evolution of the dust that tends to reduce (p15 l16)*

Response

Our comment in the original draft page 15:L16 concerns other analysis which implicate long term trends in SHL temperature to that in WV, but do not include dust in their analyses. We simply aimed to point out that this should not be neglected. Our paper is not concerned with resolving long term trends in dust over the SHL so we do not include plots of long term satellite derived AOD over the SHL.

Major Comment d.

1. *Some figures are not readable*

Response

Unreadable figures corrected.

Minor Comments

1. *P2 l11 the authors should mention this reference: Lavaysse, C., Flamant, C., Evan, A. et al. Clim Dyn (2016) 47: 3479. doi:10.1007/s00382-015-2847-z*
   Response: Reference included, P2:L11 and reference section page 18: L32.
2. *P6 l4; the two phases mentioned are not so clear.*
   Response: These two phases are previously stated on original draft page 4:L40 and page 5:L1
3. *P6 l19: title of subsection 3.2 not clear, please rephrase*
   Response: changed to 'RT sensitivity experiments to choice of inputs', now moved to supplementary material.

4. *P6 l24: optimal to what?*

   Response: Optimal configuration means model configured to produce results closest to observations.

5. *P6 l37-38; how do the authors conclude the Ceres measurements are uncertain and that explain the large RMSE? The term RMSE refers to a reference (usually observations) that are considered as the correct value. Here, I do not understand what is the reference and how they can conclude that. Please clarify. Also the term RMSD (difference) should be more appropriate*.

   Response: We do agree with the reviewer's comment that RMSD is comparison of modeled versus observation. From the data we have CERES is considered correct, despite its limitations as with any observation, can be used to measure the error modelled variables.

   Changes Made: RMSE changed to RMSD in all occasions.

6. *P6 l39-40: the authors provide some results without explanations, what are these results (mean =...) and please clarify the conclusions/interest of this point?*

   Response: Rephrased, point of interest described in section 5

7. *P7 subsection 3.2.2 I recommend to put the first part of the paragraph in the introduction section and the result in supplementary material.*

   Response: Some of the information and results on optical properties of dust is now moved to section S1 of supplementary material.

8. P8 l1: Section 4.1 is correct?

   Response: Corrected

9. *P8 l11: Is it necessary to use this acronym?*

   Response: Acronym definitions summarized in table 2. To be consistent throughout the paper, we found it necessary to use acronym.

10. *P8 l27: Section 3.1 is correct?*

    Response: corrected, for the details look at response to Major comment a.

11. *P11 l7-8: longwave and shortwave are equal*

    Response: TOA SW DRE of dust is small, whereas LW has a net warming effect at TOA(less LW escaping out of atmosphere due to dust.)

12. *P12 l36-37: The SHL is measured in between 925 and 700hPa, not at the surface. Do the authors conclude there is a cooling of the SHL intensity due to the water vapor?*

    Response: Here we are discussing the immediate radiative effect of dust and water vapour. But the net effect may not be cooling as the feedback resulting from surface warming in the LW and thus more sensible heat flux could result in net warming of the atmosphere which needs further investigation using regional climate models that include the feedback processes.

13. *Figures : For all the figures, please add the caption under the figures*

    Response: All changes are made to the figures according to the given recommendation.

Response to Referee Comment (RC) from Anonymous Referee #1

1. *This paper used field experiment data at BBM in southern Algeria from June 2011 and a radiative transfer model to calculate the effects of dust and water vapor on radiation budget both at the surface and the TOA in order to understand the radiative processes within the SHL during summer. Generally, the manuscript is straightforward*

and well organized. However my main concern is that some of the input data for the RT model may cause large uncertainties that are helpless to fill the research gaps as the authors mentioned in the introduction.

Response

We fully recognise the challenge of adequately constraining the input data to the RT model in this region, where observations are sparse and as a results reanalyses models have limited assimilation of observations. This is indeed a challenge and one which the Fennec project set out to address. In using Fennec data we therefore utilise the best available data for our RT simulations. Moreover, we undertake a very comprehensive analysis of the sensitivity of radiative heating to uncertainties in those input field not directly measured during Fennec. Indeed reviewer 1 felt that this model configuration section was too comprehensive to be included in the main paper! So we believe we have addressed the issue of data input uncertainty as thorough and comprehensive manner as could be reasonably expected. This is now included in the supplementary material section so as not to distract from the core hypotheses the paper sets out the test.

2. *For example, dust can absorb thermal infrared radiation, the night time AOD estimated from the nephelometer, which measures aerosol extinction coefficient near the surface, could induce a large error without an accurate aerosol extinction profile.*

Response

Lack of complete input data is one of the challenges in the study of radiative effect of aerosols. Because of this, there is always assumptions or approximations to overcome the arising difficulties. Using surface nephelometer measurements to estimate night time AOD will not significantly affect our result. This is because there is only LW forcing at night which is in general smaller compared with SW forcing. Besides researchers practically use uniform dust extinction profile across the boundary layer as the difference in forcing results compared with the actual extinction profile is not small. [Liao and Seinfeld 1998, Osipov et al., 2015,]

We have also confirmed this through a sensitivity experiment to test the difference in LW radiative flux and heating rate when we use different daytime and nighttime extinction profile. We find a small difference less than 3 $W.m^{-2}$ both at the surface and TOA. The atmospheric heating rates do not change significantly when different extinction profiles are used for day and night except small difference in the lower levels by less than 0.20 $K\ day^{-1}$. We conclude in general that this will not affect what we wanted to show and hence the overall result of the paper.

3. *Reanalysis data generally has poor representations of clouds and their properties. However, the authors selected clouds properties from the reanalysis. These could directly affect the reliability of the model results.*

Response

This was also our concern at the beginning of this research work as we understand the limitations of cloud representations in models. We could have undertaken the RT experiments only in clear sky mode as many other authors choose to do. We do include clear sky only experiments but we complement these with all sky

experiments to provide a more thorough and comprehensive analysis, from which we compare observations of TOA fluxes in which cloud screening is problematic. Our all sky RT experiments use what we feel is the best available 3-D information on cloud, that comes from the reanalysis models. Alternative cloud profiles for RT models simulations is not available. It is totally expected that our results will bring error due to cloud under (or mis) representation. We discuss this on Page 9: L14-20 of corrected draft and page 3:L1-5, L14-16 of supplementary material. However, we stand by our analysis not least because comparison of the errors in the all sky vs clear sky RT results actually provide some first order indication of the error on radiative budget due to underestimated cloud in reanalysis dataset. We have included a clearer and more explicit caveat regarding the limitations of the cloud fields in our experiments and note the need for further work in this area.

Changes Made

Page 3:L14-16 of supplementary material.

4. *Sections 2 and 3 are a bit long. I would recommend to combine and simplify this part.*

Response

This part has been restructured in a more clear way (please refer to the comment of reviewer 1, reviewer #1 Major Comment a #1.)

Changes Made

Refer to the response of reviewer #1 Major Comment a #1 for the simplified layout of the paper.

5. *What the authors concluded cannot be totally supported only from the radiative forcing and heating rate calculations.*

Response

Reviewer #1 also raised this comment. Please refer the responses made to reviewer #1, Major Comment C #2

6. *The manuscript also need a thorough editing. Some typos and confusing expression make the text difficult to follow at times.*

Response

Manuscript thoroughly read and corrections made to typos.

Response to Referee Comment (RC) from Anonymous Referee #2

Major Comments

1. *Error Analysis: The authors spend a good bit of time estimating uncertainty in their modeled fluxes via comparison to satellite retrieved fluxes. However, when it comes to the data analysis, these uncertainties are not taken into consideration. I think it's great that the authors have a handle on the RT model errors, but I think it would be far more useful to carry those uncertainties throughout the entirety of Section 4. Doing so would make the paper and results much stronger and would afford the community opportunity to make a more precise comparison between yours and future dust forcing estimates.*

Response

We agree the importance of including error analysis despite we have reduced the uncertainty using sensitivity experiments. This is addressed qualitatively to some extent in section 4, i.e. error associated with the uncertainties in the input.

Changes made

Additional information quantitatively expressing the error in flux calculation associated with uncertainties in some of the input data is provided. Page 8 L25-28 and L37-39.

2. *Radiative Transfer Model. To generate the mie coefficients the authors use two different size distributions (Dubovik and Ryder) but the same index of refraction. However, what's the source of the refractive index? The authors conclude that the Dubovik size distribution is more representative of the actual size distribution based on a comparison of the model and observed/retrieved fluxes. However, it is completely possible that the index of refraction used here also biased. For example, it's possible that the Ryder distribution is correct but doesn't produce enough SW dust forcing because the MEC is too low at the appropriate size parameter, thus the forcing in the SWE for Dubovik would better match observations because it's biased towards smaller particles. At any rate, my only point is that you have two degrees of freedom and you can't say conclusively that one size distribution is more representative than another one b/c the index of refraction isn't constrained.*

Response

We agree that the refractive index may cause uncertainty in the flux calculations especially in the SW absorption. It is also interesting to test the sensitivity of radiative flux to refractive index. In general for a given size distribution of dust, when refractive index is increased net SW heating will increase and net LW cooling will increase to a lesser extent. This however is a complicated function depending on the surface albedo and cloud. (Liao et al., 1998). Here we used recent measurements for dust refractive index over the Sahara (Ryder et al., 2013) which is function of the composition of dust particles, independent of the size distribution. It could be possible that if we reduce the refractive index, the SW heating will reduce in Ryder distribution, which is the biggest discrepancy compared with satellite measurement. But we haven't made sensitivity test as we have measured refractive index.

3. *RT Model: The authors state that the vertical profile of the dust mass mixing ratio is adjusted so that for a given*

MEC the AOD matches observations. Is the profile linearly scaled by a single value to match the observations? Is a single coefficient derived for all cases or is this done independently for each RT simulation?

Response

To be clearer, first an average extinction profile is derived from CALLIOP and this profile is used to derive the extinction profile at each time step, i.e. the average profile is adjusted to match the measured AOD from AERONET. So to answer the question, for each RT calculations independent extinction profile is derived.

4. *Flux comparisons: It the text it is not clear if the flux comparisons are performed in a robust manner. For example, why are monthly mean fluxes from CERES compared to the observations and output from the model? The proper way to conduct the comparison with CERES would be to access the daily nighttime and daytime data and then sub sample the observations/RT model output/GERB retrievals in order to conduct an apples-to-apples comparison. The authors acknowledge this (Page 9 line 35) so it's puzzling why a more thorough analysis wasn't performed. This approach includes the task of making comparisons to the reanalysis data (again, authors note that interpolating MERRA surface temperature may be biasing the flux comparisons). Furthermore, more insight would likely be gained by comparing the clear-sky fluxes only, since cloud forcing is not important to the study.*

Response

An important aspect of this study that needs to be noted is it is intended to provide season (one month) study of the radiative budget and sensitivities to water vapour and dust variability over the Saharan heat low. In order to do so we have used the best available input dataset through sensitivity experiments. It is useful to carry out comparison of the radiative flux at the time steps of CERES data (which is twice per day) as the referee suggested. We have actually made comparison of RT model outputs with CERES data with the respective time step to derive RMSE. This is presented on page 9 line 21(corrected draft). This will give us a good picture of the uncertainties of model simulations. However further comparisons using average of two time steps per day will not enable us to achieve the target we put at the outset.

To compare simulated flux with observation, GERB data is used. Further reanalysis data is also used which is available daily and thus used the same days as the RT model simulation days. CERES data is not used to compare simulated flux except for sensitivity experiments and estimate cloud DRE. We understand that using month mean CERES clear sky and all sky flux will bring some error but it will give us first order estimate of cloud DRE over the region. This will help emphasize need to improve the error on the radiative budget due to underestimated cloud in reanalysis dataset despite the challenges in making these comparisons.

5. *Flux comparisons: Tables and Figures. There are too many tables and the main figure (9) for this section is not particularly useful. Firstly, the tables are cumbersome and don't communicate the main results well (for example, color could be used to indicate if RT model output or reanalysis output is biased high or low in comparison to surface obs or satellite retrievals. In addition, the flux comparison Fig 9 are tough to interpret because the annual cycle is included. A better way to do this is to have one plot comparing the mean annual cycles, and another comparing the anomalies.*

Response

We agree to remove Table 5 since the information on this table is also found in Tables 2 and 3(corrected draft). An additional table is moved to the supplementary material.

Colours included on the wDwC results in tables 3 and 4(corrected draft Tables 2 and 3) red indicating model results overestimated and blue indicating model results underestimated compared with observation.

Some of the figures were corrected based on referee #1 and reviewer's comments. Figure 9(also Figure 6) is corrected and it is easier to read. We therefore keep it as it is. But have also made additional plot using anomalies but we put it in the supplementary document. See also page 9 L18-20.

Changes made

Table 5 removed
Colours used on column 6 of table 2 and table 3
Additional figure included in supplementary material page 3, figure S2

6. *Forcing efficiencies for dust and CIWV should also include the 95% confident interval from linear regressions.*

Response

We agree that the regressions should be expressed to 95% confidence level. All the regression results are expressed within the 95% confidence interval.

Changes made

These are included in section 4.2.1(page 10-11) and section 4.2.2(page 12) on the corrected draft.

7. *Figure 12 and 16 are not interesting. Consider including observations here as well (at least for TOA). BTW - CERES produces surface flux products. These could be folded into the analysis as well.*

Response

Here the plots are made using daily averaged variations in dust AOD or water vapour. That is dust AOD (and CIWV) is increased linearly in each RT run. This is a theoretical work designed to investigate the sensitivity of dust and water vapour on the radiation budget. There is no such observational data, at least at one particular point which is the observational data we used here. This can be tested for a number of grid points of Satellite observation to see sensitivity of radiation to AOD variation (e.g Young et al., 2009). However this is not the objective of this study and thus it is not included.

8. *Figure 17 is impossible to read/interpret, and I don't even wear glasses (yet)! Please consider a more simple and straightforward way to describe the vertical sensitivities. A good rule-of-thumb would be to only include in the plot information that you actually describe in the text.*

Response

Figure made easier to read. Additional explanation regarding the figures provided

Changes made

Now we put the two panels of figure 17 as independent plots, Figure 16 and Figure 17 in the corrected draft. Statement added on page 13, L18-19.

Minor Comments

1. *Individual panels of the figures should be labeled as a,b,c,…*

Response

All figures prepared accordingly

2. *Figure 5: This figure is not very useful in terms of understanding the relationship between the AODs and IWV. Can you please just replace with one or two scatter plots?*

Response

We used SEVIRI AOD to show that there are cases where AOD is missed in AERONET which we suggest to be due to confusing dust with cloud. This we believe is important to show there are cases where dust might be missed in AERONET. We have complemented this using nephelometer measurements.

3. *Figure 6. If the authors removed the diurnal cycle from this plot we'd have an easier time interpreting the magnitude of the biases. As it is presented here, the magnitude of the differences are small relative to the magnitude of the diurnal temperature changes, making it difficult to interpret the results.*

Response

Figure 6 is now made easier to read and thus we keep it as it is. In addition we put the anomalies in the supplementary material. Additional information included in the supplementary material SP2 L:21-22

4. *Page 9, Line 2: You write "Dubovik Optical Properties" do you mean optical properties generated using the size distribution from Dubovik and the index of refraction that you've been using up to now (that hasn't been referenced)? It's just not clear.*

Response

Restated. Now on page 7 line 10 and 14.
Refractive index used comes from measurement. It is now made clear, Citation included, page 5 line 36

5. *Page 12, Paragraph starting on line 28: The finding that IWV and AOD contribute approximately equally to variance in the radiative budget is by far the most interesting (and new) finding reported in the paper. Why not take a little more space to flesh this out a bit? And please include the uncertainty estimates.*

Response

We agree this is an important point. Additional statement highlighting the significance of dust on controlling the radiative budget is included. Page 13 Line 4 of corrected draft.